SKBF
KBS
TEKNISK
RAPPORT
83-04

Stability of bentonite gels in crystalline rock – Physical aspects

Roland Pusch

Division Soil Mechanics, University of Luleå
Luleå, Sweden, 1983-02-20

SVENSK KÄRNBRÄNSLEFÖRSÖRJNING AB / AVDELNING KBS

POSTADRESS: Box 5864, 102 48 Stockholm, Telefon 08-67 95 40

STABILITY OF BENTONITE GELS IN CRYSTALLINE ROCK - PHYSICAL ASPECTS

Roland Pusch

Division Soil Mechanics
University of Luleå
Luleå, Sweden, 1983-02-20

A list of other reports published in this series during 1983, is attached at the end of this report. Information on KBS technical reports from 1977-1978 (TR 121), 1979 (TR 79-28), 1980 (TR 80-26) and 1981 (TR 81-17) is available through SKBF/KBS.

STABILITY OF BENTONITE GELS IN CRYSTALLINE ROCK – PHYSICAL ASPECTS

LULEÅ FEB. 20 1983
DIV. OF SOIL MECHANICS
UNIVERSITY OF LULEÅ

ROLAND PUSCH

CONTENTS

		Page
	SUMMARY	
1.	OBJECTIVE	1
2.	THE CLAY GEL	2
	2.1 General	2
	2.2 Particle size distribution	2
	2.3 Major features of the gel migration	4
	2.4 Microstructural features of the expanded clay gel	5
	2.4.1 The expansion process	5
	2.4.2 Particle interaction in expanded montmorillonite	9
	2.4.3 Gel-sol transitions	14
	2.5 Comments	16
3.	THE SYSTEM OF ROCK JOINTS	17
	3.1 General	17
	3.2 Orientation	17
	3.3 Surface characterization	18
	3.4 Frequency, extension, and cross-linking	20
	3.4.1 Frequency	21
	3.4.2 Extension	23
	3.5 Aperture	25
	3.6 Rock joint space, "rock porosity"	26
	3.7 Simplified model	
	3.7.1 Joints	27
	3.7.2 Water flow	29
	3.7.3 Conditions around a deposition hole	29
4.	GEL MIGRATION	31
	4.1 Premises	31
	4.2 The basic mechanisms	31
	4.2.1 "Free expansion"	32
	4.2.2 "Poiseuille", extrusion case	37

		Page
4.3	Experimental	42
4.3.1	Pilot tests	42
4.3.2	Main test series	45
4.4	Conclusions	57
5.	EROSION	58
5.1	Physical aspects	58
5.2	Particle bond strength	59
5.2.1	Introduction	59
5.2.2	Viscometer tests	61
5.2.3	Evaluation of particle bond strength	66
5.3	Drag forces	70
5.4	Pinhole tests	73
5.4.1	Equipment	73
5.4.2	Test procedure and program	74
5.4.3	Results	78
6.	DISCUSSION, CONCLUSIONS	81
6.1	Bentonite loss by clay expansion	81
6.2	Bentonite loss by erosion	83
6.3	Effect of clay migration on rock stability	84
6.4	Beneficial effects of clay migration from deposition holes	86
7.	ACKNOLWLEDGEMENTS	87
8.	REFERENCES	88

SUMMARY

A first estimate of the possible penetration of bentonite from deposition holes with radioactive canisters into rock joints traversing the holes was made a few years ago as part of the KBS research. It showed the importance of the geometrical properties of the joints and of the porewater chemistry with respect to the dispersibility of the expanding clay, but did not yield quantitative measures of the bentonite loss. The present, extended study comprises a derivation of a simple rock model as a basis for calculation of the penetration rate of bentonite and of the groundwater flow rate, which is a determinant of the erodibility of the protruding clay film. This model, which is representative of a gross permeability of about 10^{-8} - 10^{-9} m/s, implies a spectrum of slot-shaped joints with apertures ranging between 0.1 and 0.5 mm. Using this model and an earlier derived physical model for the clay penetration it is concluded that less than 2% of the highly compacted bentonite will be lost into traversing joints in 10^{6} years. A closer analysis, in which also Poiseuille retardation and short-term experiments were taken into account, even suggests that the penetration into the considered joints will be less than that. The penetration rate is expected to be 1 decimeter in a few hundred years; probably, the widest joints of the model will be filled with clay to within about 2 decimeters from the deposition holes in the same period of time.

The risk of erosion by flowing groundwater was estimated by comparing clay particle bond strength, evaluated from viscometer tests, and theoretically derived drag forces, the conclusion being that the maximum expected water flow rate in the widest joints of the rock model ($4 \cdot 10^{-4}$ m/s) is not sufficient to disrupt the gel front or the large individual clay flocs that may exist at this front. This hypothesis was tested by conducting pinhole experiments with a somewhat more sophisticated technique than that

applied in conventional earth dam design. Although the expected flow/erosion relationship was not explicitely obtained, these experiments still support the conclusion that erosion will not be a source of bentonite loss.

A "worst case" scenario with a shear zone being developed across deposition holes is finally considered and in addition to this, the conditions in the fracture--rich tunnel floor at the upper end of the deposition holes are also analysed. This study shows that even if the rock is much more fractured than "normal conditions" would imply, the bentonite loss is expected to be very moderate and without substantial effect on the barrier functions of the remaining clay cores in the deposition holes.

1. OBJECTIVE

The protective effect of the very dense bentonite on the metal canisters with the highly radioactive waste according to the KBS concept, depends on two major conditions with respect to the bentonite:

1. Chemical stability is required, in principle, since it determines to what extent the physical properties are preserved
2. Physical stability in the sense of a reasonably well preserved density is required. This is because the permeability, ion diffusivity, and bearing capacity are strongly dependent on the bulk density

The chemical stability will not be dealt with in this report, which will instead be concerned with a possible bulk density reduction of the bentonite in the deposition holes by expansion into joints extending from the holes (Fig. 1), and by eroding groundwater flow through the rock which confines the clay core. Such erosion primarily attacks the bentonite gel which forms the front part of the clay migrating from the highly compacted core. Theoretically, the erosion might also affect the dense clay core, but in practice this will not take place as can be inferred from this report. In addition, the self-sealing power of bentonite that enters rock joints will be discussed.

The study comprises an examination of the physical processes involved in the migration as well as in the groundwater erosion, based on theory as well as on experiments. Practical consequences are discussed in the final chapter.

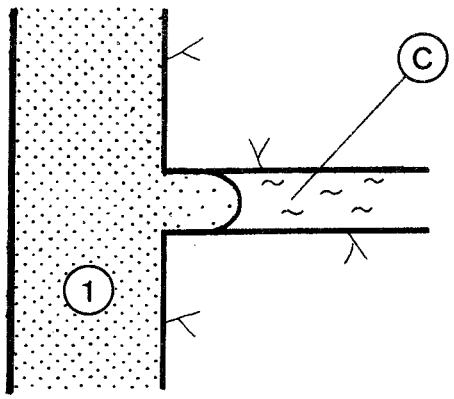

Fig. 1. Clay gel migrating from a deposition hole into an adjacent joint. C) Water flowing parallel to the protruding clay gel. 1) Highly compacted bentonite forming the clay core.

2. THE CLAY GEL

2.1 General

The blocks of highly compacted bentonite, which are applied in the deposition holes, have a tremendous swelling potential due to the low original water content (w~10%), which corresponds to approximately 50% degree of water saturation. The water uptake from the rock and the associated swelling causes a penetration of the bentonite into open joints, the front of the advancing clay being characteristically very soft. The penetration rate is a function of the density and of the joint width, while the erosion of the clay gel depends on its shear strength as well as on the flow rate of the water in the joints, this rate being determined by their aperture and by the local hydraulic gradients.

2.2 Particle size distribution

While the most obvious granulometric feature of commercial bentonite powders of the MX-80 type is the sphere-shaped, very dense aggregates which are silt/

/sand-sized, such powders can be completely dispersed to form an isotropic sol of individual flakes with a thickness of about 10Å. This requires a particular chemical composition of the water in which the clay is dispersed. Standard sedimentation analyses show that about 85% of the particles have an equivalent Stoke diameter (d) of less than 2 μm. The size distribution of the individual platelets of Wyoming bentonite determined by electron microscopy is illustrated by Fig. 2; a suitable definition of particle size and shape being shown in Fig. 3. It is safely estimated that the large majority of all the dispersed platelets of this particular clay are smaller than 0.5 μm.

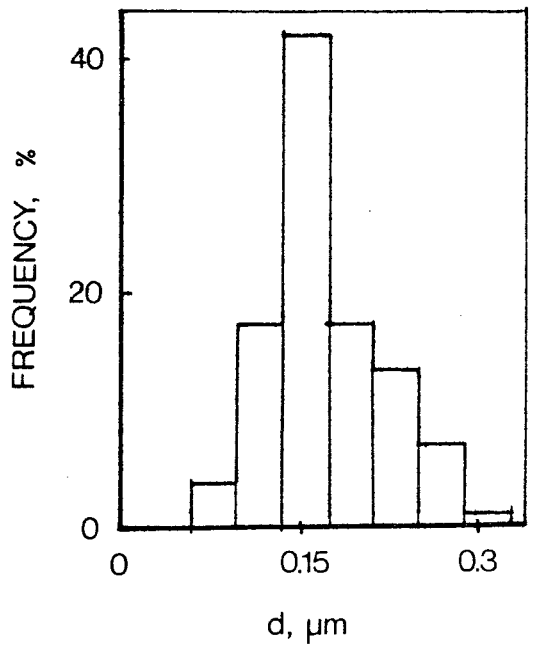

Fig. 2. Particle size distribution of Wyoming bentonite. The histogram represents a bentonite sol that was centrifuged to remove coarser particles [1].

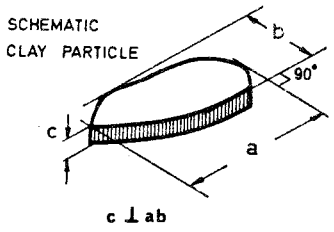

Fig. 3. Definition of particle size and shape of clay particles. d in Fig. 2 is roughly the average of a and b.

2.3 Major features of the gel migration

The water uptake in the dense bentonite clay core in a deposition hole produces expansion of the clay so that a firm contact is established with the confining rock. The swelling potential leads to a continued expansion of bentonite clay from its confinement into rock joints. This penetration is the net effect of two different mechanisms:

1. Swelling due to water uptake ("reversed" consolidation)
2. Retardation due to wall friction effects

The macroscopic process is dealt with in detail in a subsequent chapter; here we will be concerned with the physical background including particle interaction and structural reorganization covering the entire range from the highly compacted state of the bentonite core to the very soft front of the penetrating gel which represents the ultimate state of the expansion (Fig. 4).

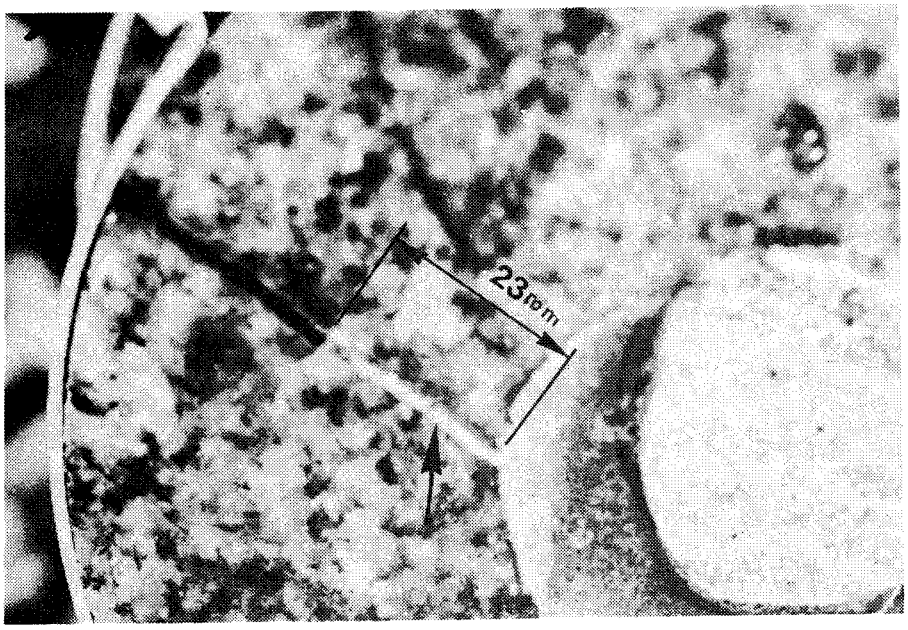

Fig. 4. Photo of bentonite clay (arrow) having entered a 1.5 mm wide joint extending from a central clay core (borehole plug). The average water content of the filling is about 120%; 30-35% in the inner part. The penetration depth of the relatively stiff part of the clay filling is 23 mm.

2.4 Microstructural features of the expanded clay gel

2.4.1 The expansion process

The freshly compacted bentonite, which has a bulk density of about 2.1 t/m^3 and a water content of the order of 10%, is characterized by the inhereted fine--structure of the raw material, i.e. the bentonite powder. This yields an aggregated microstructural framework with very small intra-aggregate particle spacings and with fairly large pores. In the course of water saturation the aggregates expand and, if given sufficient time, most of the larger voids will be partly or entirely filled by a clay gel emerging from the expanding aggregates (Fig. 5), [2]. In the deposition holes where the bentonite is confined by rock

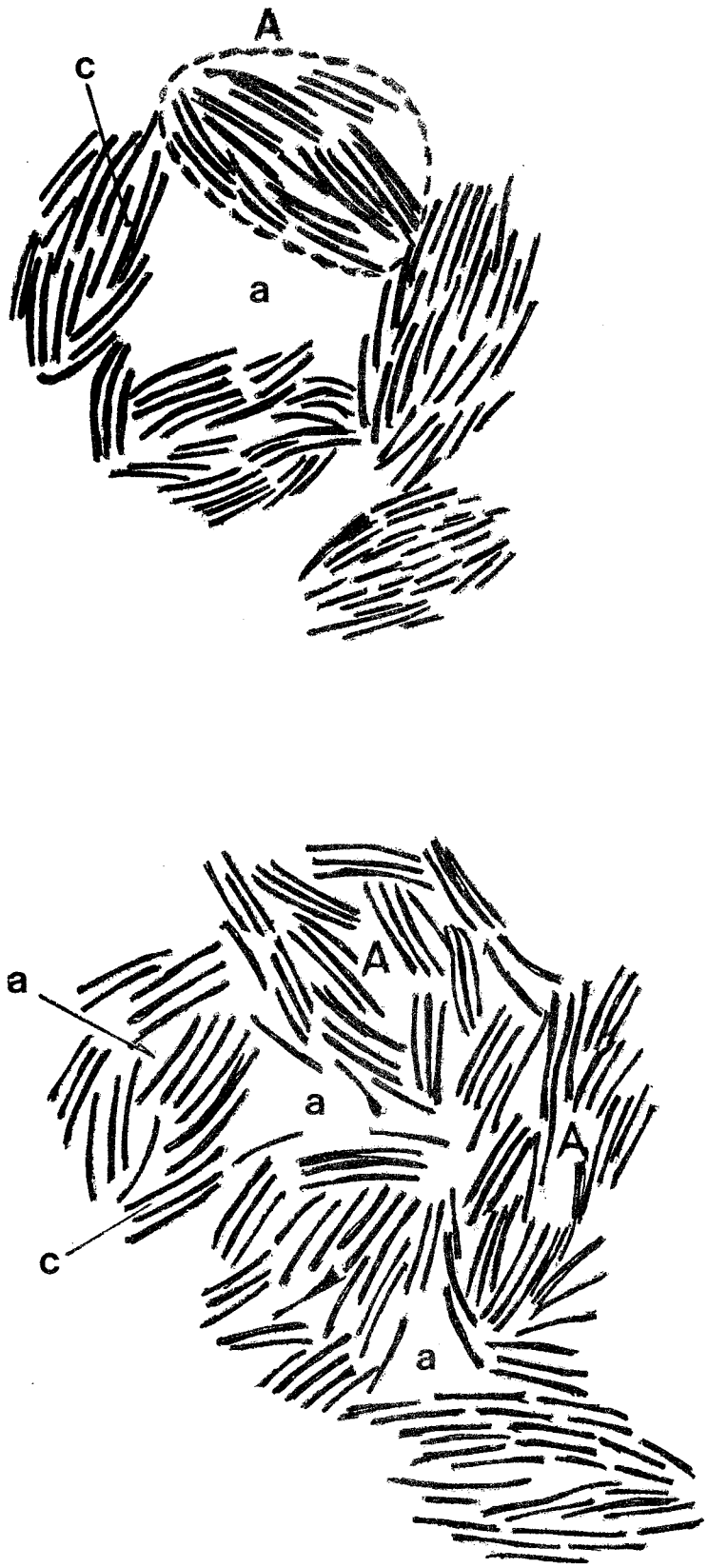

Fig. 5. Schematic picture of the grouping of Na montmorillonite crystallites in freshly compacted bentonite [upper picture, (A) representing an aggregate, a) an interaggregate void and c) an intra-aggregate space] and aged, homogeneous bentonite (lower picture).

and the swelling therefore very small, a condition of considerable isotropy and homogeneity will eventually be reached. In principle, the initial condition of parallel orientation of the thin laminae in the individual aggregates will be preserved while the spacing of the laminae will be increased. Applying the figure 800 m^2/g of the specific surface area of Na montmorillonite and disregarding void inclusions in the clay matrix, we arrive at the average free distance between the basal planes of the laminae given by Table 1.

Table 1. Distance (a) between basal planes of parallel montmorillonite crystallites in water saturated bentonite.

a	w[1]	ρ_m[2]
Å	%	t/m^3
3.7	14.8	2.21
4.6	18.5	2.13
5.5	22.2	2.06
6.5	25.9	2.00
7.4	29.6	1.95
8.3	33.3	1.90
9.3	37.0	1.85
13.9	55.5	1.68
22.3	89.0	1.50
54	216.0	1.25
148	593.0	1.10

[1] Water content

[2] Bulk density of water saturated clay

The distance a is not, in fact, a continuous function of the water content. Data have been published of the lattice expansion of Na montmorillonite that clearly show the discrete character of the c-axis spacing [3], [4]. Various physical explanations of this phenomenon have been given for possible crystal

lattice models which imply different modes and coupling of the water molecules to the basal planes of the crystallites. The essential thing is that the hydration stages seem to be relatively unaffected by the pore water chemistry for water contents lower than about 35%, which corresponds to 3 ordered water molecule layers [4]. Similarly, the pore water composition is hardly a determinant of the swelling pressure in this water content interval [2], which suggests that the "disjoining" pressure exerted by the interlamellar water is primarily due to its structured nature, i.e. to the tendency of surface-near water films to "crystallize". There are reasons to believe that the stability of the water lattice drops rapidly with increased basal spacings and that it is of negligible importance as to the swelling pressure when the free distance between the basal planes exceeds 12-15 Å, i.e. when the water content exceeds 50-70% [5]. This also means that if free expansion can take place, the lamellae are free to move in relation to each others, i.e. to deviate from the parallel arrangement that is typical for low water contents. Experience shows that a sample of Na montmorillonite which is submerged in water expands to many times its original volume, while Ca montmorillonite shows a limited swelling only. This is associated with different microstructural patterns, the Na version being characterized by an open, irregular particle arrangement and the Ca version still retaining, more or less, the initial domain-like fashion (Fig. 6). The reason for this difference is manifold, one explanation being that the sodium ion is associated with more water molecules than the calcium ion, which means that the Na montmorillonite domains become dispersed. Once the interlamellar distance becomes large enough to allow for the development of electrical double-layers, further expansion is enhanced.

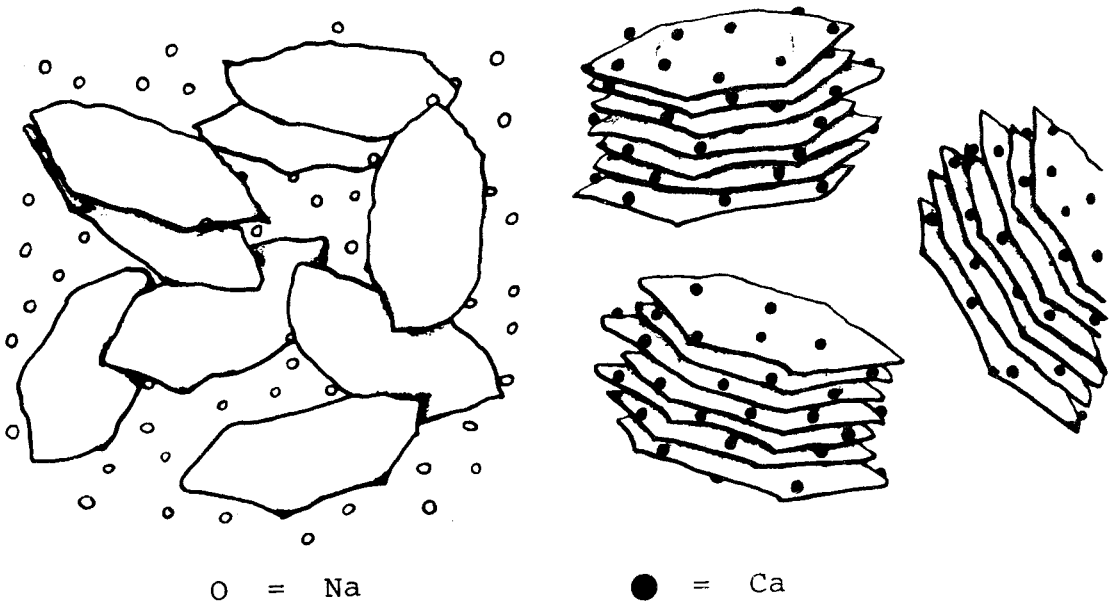

Fig. 6. Left: Irregular type of particle association in Na-saturated montmorillonite clay. Right: Domain-type arrangement of crystallites in Ca-saturated montmorillonite. [After FAHN].

2.4.2 Particle interaction in expanded montmorillonite

When the lamellae are no longer parallel the inter-particle force fields are changed. The degree of continuity of the particle network deteriorates and the particle bonds become weaker as a result of the expansion and, depending on the ground water chemistry, the gel may be transformed to as sol. The matter, which involves the application of colloid chemistry, has been dealt with – mainly theoretically – in various reports [6], [7]. The DLVO theory [8], which concerns the potential energy of interaction between two adjacent colloidal particles, (e.g. electrical double layer repulsion and LONDON van der WAALS attraction) has been found to be in reasonable agreement with certain experimental observations. Yet, it fails to give a complete picture of particle interaction including the rôle of mineral-adsorbed water molecules, particularly at edge-to-face or edge-to-edge association modes of the particles [9], [10]. These types of particle contact logically develop in later stages of the expansion if the gel state is preserved and they have

been widely observed by applying electron microscopy (Fig. 7).

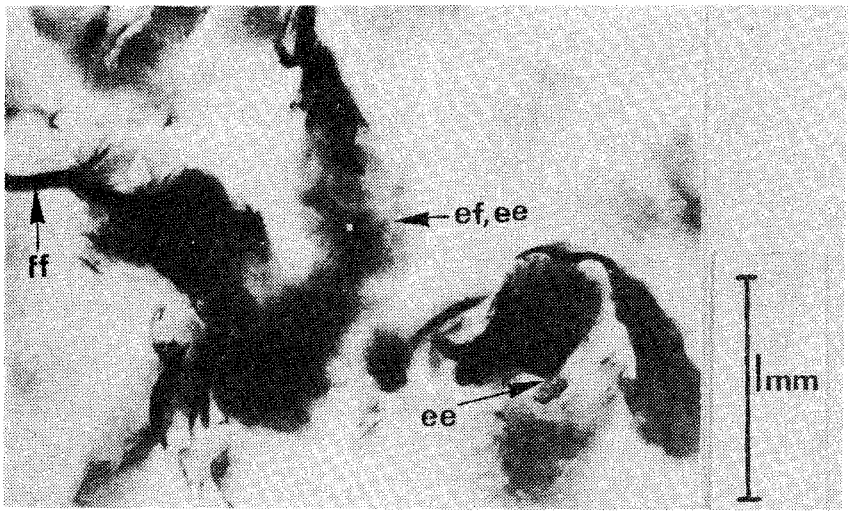

Examples of particle contacts:
ff=face-to-face, ef=edge-to-face, ee=edge-to-edge

Fig. 7. Soft Na montmorillonite gel. The line is 0.5 μm long.

It has been postulated that positive charges are present on the edges of clay plates and that this would lead to flocculation resulting from attraction between positively charged particle edges and negatively charged particle faces [9]. The part of the edge surfaces at which octahedral sheets are broken, will carry positive double-layers in acid and neutral solutions and negative double-layers in alkaline solutions. Where tetrahedral sheets are exposed positive double-layers may exist in the presence of very small amounts of aluminum ions in the suspension. Because of the slight solubility of clays a certain concentration of aluminium will always characterize clay suspensions. Thus, under appropriate conditions, the entire edge surface may well carry a positive charge. It has further been suggested that sediment volumes are influenced by the size of the hydrated ion, which decreases in the order Li>Na>K>Cs [10]. Edge-to-

-face arrangements resulting from the polarization of individual particles also arises from non-uniform distribution of surface charges [11] and density gradients in adsorbed water layers [12].

Various types of bonding mechanisms have been assumed to cause other particle associations. Thus, 1) attraction caused by an asymmetrical distribution of adsorbed cations by which simple eletrostatic bonding is effected, 2) van der WAALS forces between polarized adsorbed cations, 3) attraction forces between cations adsorbed on one particle and the lattice field of adjacent minerals, 4) attraction by the action of adsorbed polar molecules or hydrogen bonds, may all lead to several kinds of particle associations such as edge--to-edge arrangements. A schematic illustration of such a pattern, suggested by ROSENQVIST [13], is shown in Fig. 8. The latter sort of particle arrangement can result from interactions in sols or very dilute gels. Thus, the formation of a flocculation (coagulation) structure in a dilute suspension is induced by the cohesion between the colloidal particles driven by Brownian movement. The colliding particles, which are assumed to join at the least hydrophilic sites, are said to be separated by thin residual water interlayers at the points of association. An open network is promoted by an anisodiametric shape of the particles (Fig. 9). According to DERYAGIN's cohesion theory neighbouring particles are connected where the radius of curvature of the mineral surfaces is minimum, that is where the dispersing medium is most easily displaced. This implies that the flocculation structure consists of particles connected edge-wise [14].

A plausible picture of edge-to-face contacts, which is in principle valid also for edge-to-edge couplings, is given in Fig. 10. It shows the interparticle link bond through hydrogen bonds and van der WAALS bonds that develop in the two-phase system, and which contribute to the strength of the contact which may primarily be due to electrostatic and chemical bonds.

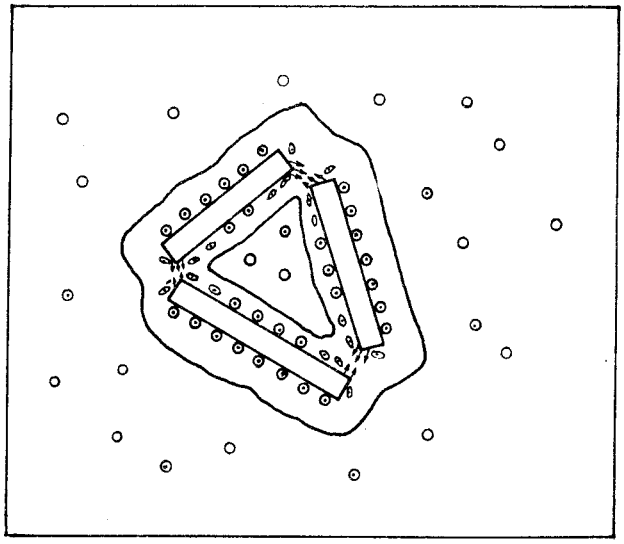

LEGEND:

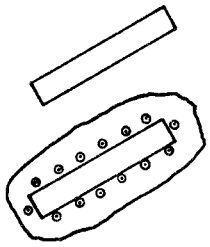

SECTION THROUGH A CLAY MINERAL

CLAY MINERAL WITH CATIONS AND FIXED WATER FILM

⊙ (+) CATION

o (–) ANION

Fig. 8. Edge-to-edge coupling through polarization of adsorbed cations [13].

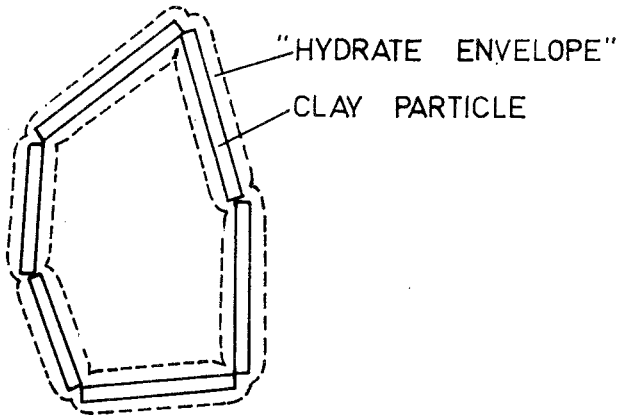

Fig. 9. "Recticular" structure in very soft clay gels.

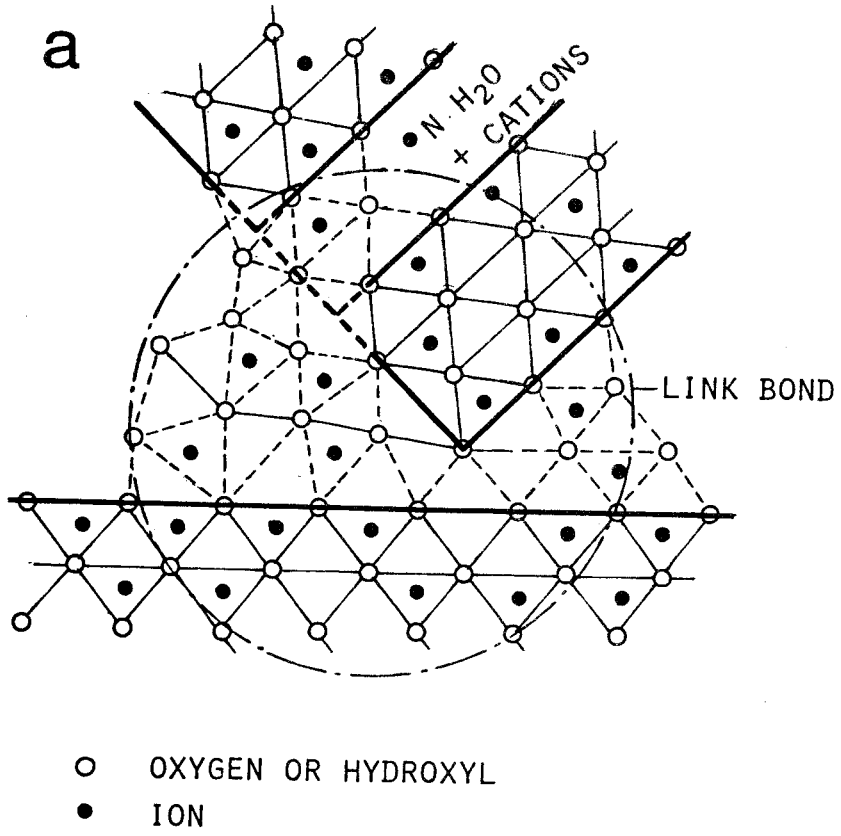

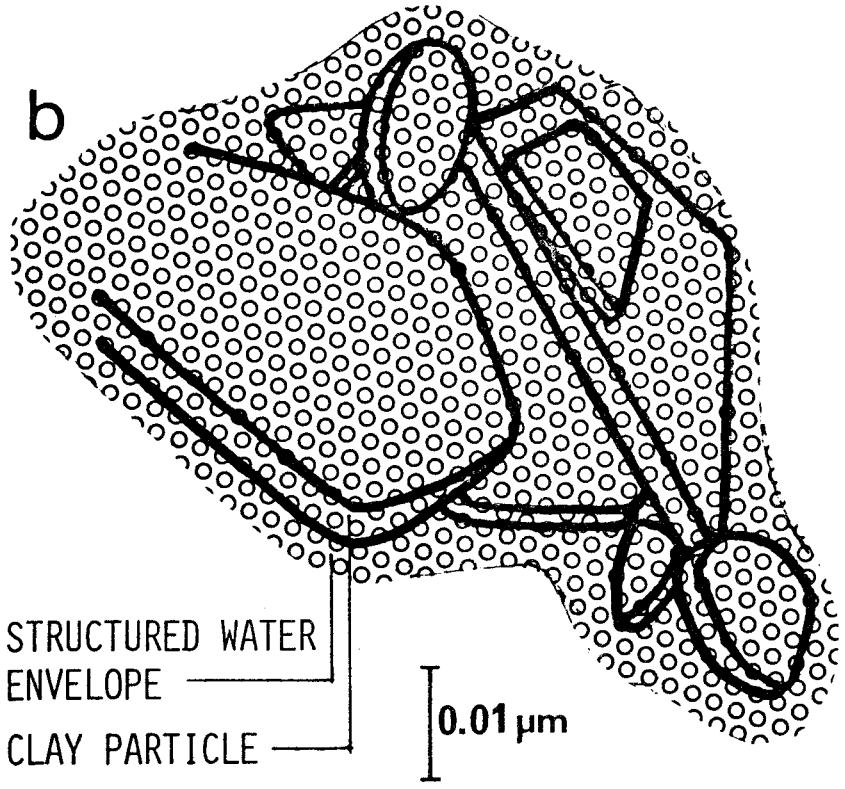

Fig. 10. General character of edge-to-face contacts of clay particles. a) Mineral/water structure [15], b) Particle floc with structured water envelope [16].

2.4.3 Gel-sol transitions

The gel character provided by the continuity of edge--to-face coupled particles may be lost depending on the salinity and pH conditions in the water. Thus, high pH may reduce the positive charge of the edges and lead to dispersion, and similar effects also result from low electrolyte contents. Experiments with kaolinite have in fact indicated that the sediment volume and therefore the particle bond strength have minima at a certain salt content. Numerous reports on the similar, very obvious dependence of the shear strength of dilute Na montmorillonite on the salinity of the water, have been published [17], [18]. Fig. 11, which serves as an example of the importance of the electrolyte content for the gel strength, shows that Na montmorillonite gels with very high water contents –

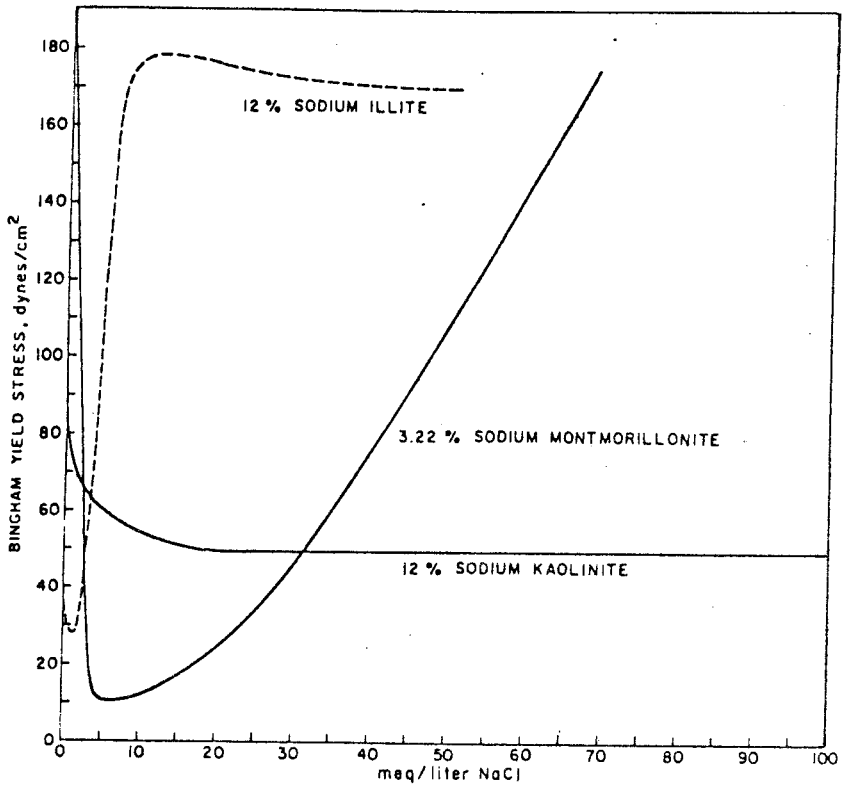

Fig. 11. BINGHAM yield stress of clay suspensions as a function of the salt concentration [18].

– the graph represents a montmorillonite gel with a water content of about 3300% – suffer a drastic drop in strength at certain low electrolyte contents.

Recent experiments with freely swelling Wyoming bentonite (MX-80), which is rich in montmorillonite and has sodium as main adsorbed cation, have verified that gel stability depends on the groundwater salinity [19]. These experiments in which clay gels with 15% concentration ($1.5 \cdot 10^5$ mg/l), i.e. with a water content of about 670%, were contacted with various solutions, gave the concentration of particles at 5 mm distance outside the original interface that is given in Table 2.

Table 2. Particle concentrations at 5 mm distance from original gel/solution interface [18].

Solution	Time after contacting	Clay conc.	Clay conc.
	days	mg/l	%
Aqua dest	7	0.1	10^{-5}
	14	0.5	$5 \cdot 10^{-5}$
$CaCl_2$, 10^{-4}M	9	0.01	10^{-6}
	14	0.5	$5 \cdot 10^{-5}$
$CaCl_2$, 10^{-3}M	7	<<0.01	<<10^{-6}
	14	0.01	10^{-6}
Synthet.ground water[1)]	14	<<0.01	<<10^{-6}

[1)] 33 ppm Ca^{2+}, 124 ppm Na^+, 7 ppm Mg^{2+}, 5 ppm K^+, being the main cations.

The experiments showed that the clay gel did actually not expand in any of the solutions and that particle release through Brownian motion or convection was insignificant except in the distilled water and the

most diluted $CaCl_2$ solution. Such dispersion was practically inhibited in the 10^{-3}M $CaCl_2$ solution and in the synthetic groundwater. Since this water contained more dissolved ions than certain representative natural groundwaters do, we need to consider the question of coagulation and particle release in greater detail. Thus, it must be expected that the Ca concentration will be as low as 10 ppm, which corresponds to a $CaCl_2$ concentration of 0.5 meq per liter or $2.5 \cdot 10^{-4}$M. This concentration is sufficient to convert a Na montmorillonite particle sol with a concentration of 0.35 g clay per liter to a calcium state, assuming the base exchange capacity to be 70 meq per 100 g dry clay, and this sol then requires only some minor additional $CaCl_2$ to flocculate [18]. Considering the fact that calcium ions occupy a certain fraction of the adsorption sites in the original state of the clay, and that magnesium and polyvalent ions are also present in the groundwater, we can safely conclude that a flocculated state will always be preserved. The most diluted form of a bentonite gel in natural groundwater will correspond to about 200-300 mg clay per liter, i.e. 0.02-0.03% or, expressed as a water content, $w \sim 3 \cdot 10^5 - 5 \cdot 10^5$%. In practice, this does not correspond to an isotropic, homogeneous mass but rather to a very open, system of more or less cohering, large flocs. Also, a faint cloud of released dispersed particles is expected to be present, its concentration probably being of the order of 0.1 mg/l.

2.5 Comments

The various interparticle forces are reasonably well defined and understood but quantitative evaluation of their net effect in the particle contacts is hardly possible on a purely theoretical base. The order of magnitude of the bond strength can be roughly estimated,

however, by considering electrostatic and van der Waals interaction of particles coupled edge-to-face, and edge-to-edge [17]. According to OSIPOV the net attractive force in "coagulation contacts", i.e. where the particles are separated by a stable hydrate film with a thickness of several tens of Å, ranges between 10^{-12} and 10^{-10}N depending on the pore water salinity and the actual pH. These figures represent conservative estimations according to this reference.

3. THE SYSTEM OF ROCK JOINTS

3.1 General

The migration of clay into the rock and the simultaneous erosive effect on it by flowing groundwater are very much dependent on the character and geometrical properties of the rock joints. Further treatment of the problem of bentonite gel behavior requires definition of the properties of the joints, which is the object of this chapter.

3.2 Orientation

Most rock masses contain planar surfaces of potential or real weakness and they come in all lengths and spacings. Usually they form sets, one of which is almost horizontal, and one very steep while there is often a third and sometimes a fourth of intermediate orientation. Also, a certain small number of completely irregularly oriented joints or fractures are always present as illustrated in Fig. 12, wich also shows the characteristic dependence of excavated rock profiles on the geometry of the joint pattern.

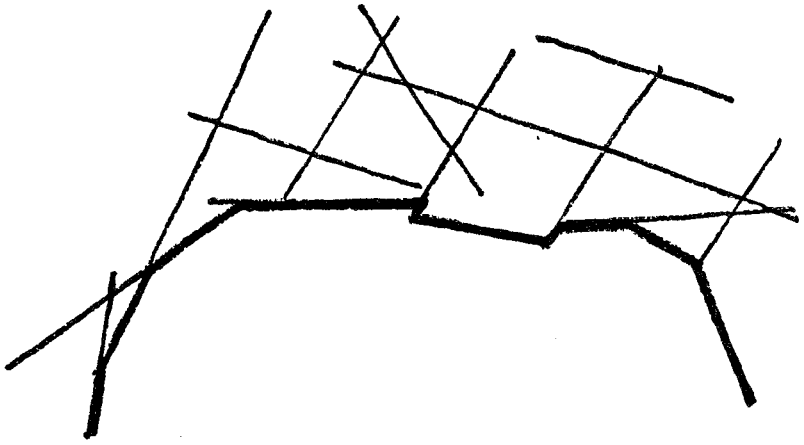

Fig. 12. Schematic picture of the roof shape of a blasted tunnel.

3.3 Surface characterization

Joints and fractures represent three major types of discontinuities with respect to the surface character:

1. Fracture plane traversing virgin rock matrix
2. Interface between different rock units, representing original bedding planes, eroded surfaces, or boundaries between host rock and intrusives.
3. Slots with fillings, such as plastic or cemented sediments (sandstone dikes etc), or coatings precipitated from hydrothermal solutions (chlorite, calcite etc).

All three types are characterized by an irregular surface topography which depends on the macroscopic structural pattern of the crystal matrix. For the present purpose they can all be considered as very rough, even in slickensides, particularly considering the common pattern of incomplete intercrystalline contacts, which create the surface topography shown in Fig. 13.

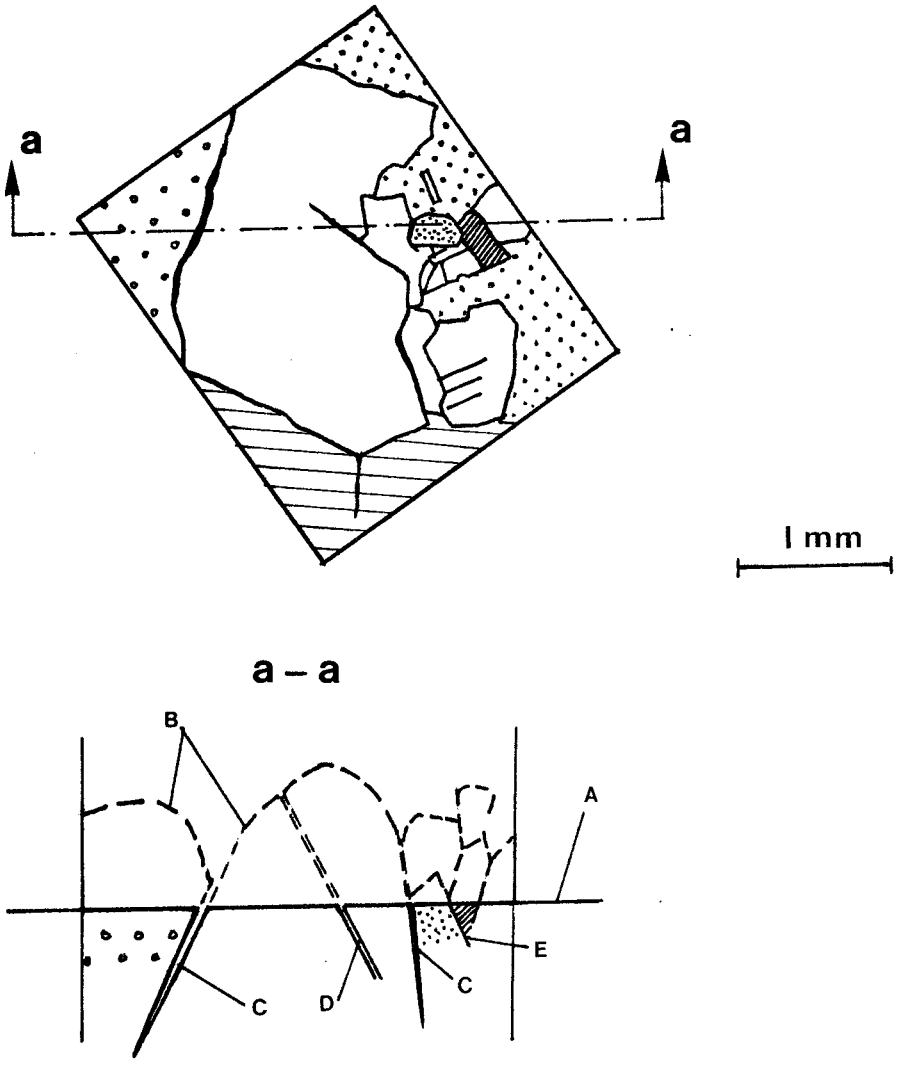

Fig. 13. Graphical interpretation of actual rock section (Stockholm granite, [20]). (a-a) represents a hypothetical cross section through the rock matrix. A) is polished surface of the 30 μm thick section for microscopy, B) actual irregular surface exposed in a joint, C) incomplete inter-crystalline contacts, D) fissure through crystal, E) tightly contacting crystals.

Joints with infilling of clastic clay-rich material have a very high surface activity. Thus, if the density of the filling is 2 t/m^3, the clay content 50%, the surface area 30 m^2/g dry clay, and the base exchange capacity 30 meq/100 g, each square

meter of the filling represents an active surface area, per millimeter joint width, of more than 20 000 m^2, its base exchange capacity being more than 200 meq. The flow resistance of such infillings is of course considerable.

Open joints coated with chlorite or micas also exhibit surface activity, the base exchange capacity being of the order of 20-40 meq/100 g of the first-mentioned mineral and 5-10 meq/100 g of the latter. It should be noticed that freshly opened fractures even through quartz and feldspars have a very high surface activity [cf. 21]. However, after a few days or weeks this activity drops considerably in connection with surface alterations forming the first phase of weathering. Calcite-coating is not surface-active but serves as a calcium source in ion exchange processes and diagenetics. Epidote also occurs as a mineralization but it does hardly contribute to the surface activity.

3.4 Frequency, extension, and cross-linking

Although being basic to rock mechanics and hydrology, generalized realistic joint models have not been developed until very recently. The required empirical basis for such derivations is actually very limited and rather crude approximations still have to be made in practical engineering with respect to the premises concerning joint widths, extensions and frequencies. The main information source used by the author in this report will be the comprehensive study of Stripa granite made by the Lawrence Berkeley Laboratory (LBL) [22], practical experience, and general basic hydraulics.

3.4.1 Frequency

Table 3 illustrates the main fracture[1] spacing distribution parameters for the Stripa granite [22]. It shows that the mean spacing of the fractures constituting the four main fracture sets is less than one meter. Actually, if all visible fractures (fissures) are considered we arrive at very small spacings (Figs. 14 and 15).

Table 3. Fracture spacing parameters of Stripa granite [22].

Set no.	Mean vertical spacing, m	Mean dip angle (°)	Normal spacing, m
1	0.73	41	0.55
2	0.50	59	0.25
3	0.32	39	0.25
4	0.42	0	0.42

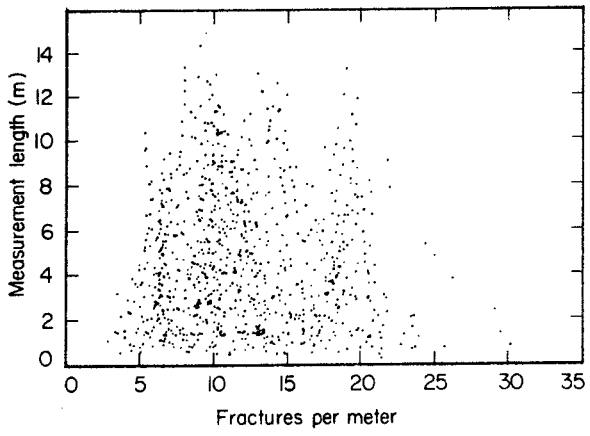

Fig. 14. Frequencies for all fractures visible in core photographs of Stripa granite [22].

[1] The LBL reports usually apply the term fracture for all discontinuities in rock. The author uses joint for clearly visible natural discontinuities, fissure for narrow, less obvious ones, and fracture for fresh discontinuities which clearly are associated with fracture due to overstressing.

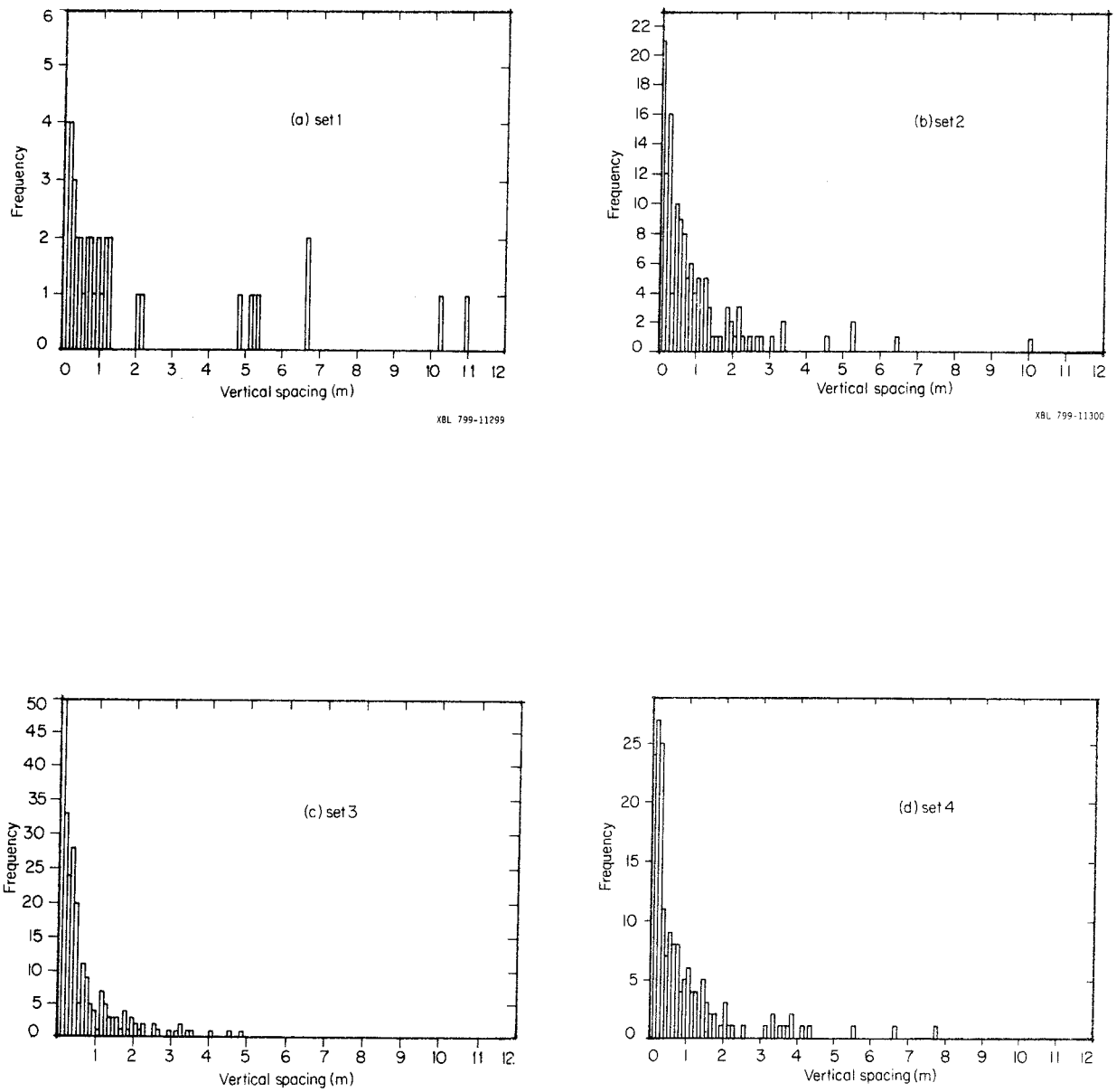

Fig. 15. Vertical fracture spacing-frequency histograms for all four joint sets in Stripa granite [22].

The fracture logs include all types of discontinuities, open and closed ones, as well as completely sealed joints. Their practical importance with respect to water flow cannot be evaluated without considering the aperture and type of filling, as well as the

extension of the various discontinuities. It is clear, however, that even if fissures as well as closed and filled joints and even incomplete crystal contacts contribute somewhat to the gross hydraulic conductivity, they do not offer a passage for expanding clay, nor do they let water through at a rate that yields erosion of the clay. Thus, only very few of the large total population of discontinuities are of interest in this context.

Experience from ordinary rock excavation activities in Sweden indicates that crystalline rock of intermediate to high quality usually has a joint spacing of more than 0.5 m, while in poor quality rock that needs reinforcement, the spacing is often smaller than 0.3 m. These frequencies, which concern clearly observable closed as well as open joints, agree well with several practical rock quality classification schemes. Clearly observable joints simply means discontinuities which are expected to influence the rock mechanical as well as hydraulic properties of the rock mass.

3.4.2 Extension

The persistence of joints, or trace lengths, was determined by LBL for the Stripa granite, the result of the measurements being collected in Fig. 16. We can conclude from the diagram that the persistence of the large majority of joints is remarkably small. Actually, only 15% of the total number of identified fractures, closed or open, persist more than 4 meters, and only about 2% have an extension of 7 m. This is of course very important for the gross hydraulic conductivity and porosity of the rock and it points, in turn, to the importance of the degree of cross-linking of the joints. At present, no practical way of expressing the latter property seems to be currently applied in practice.

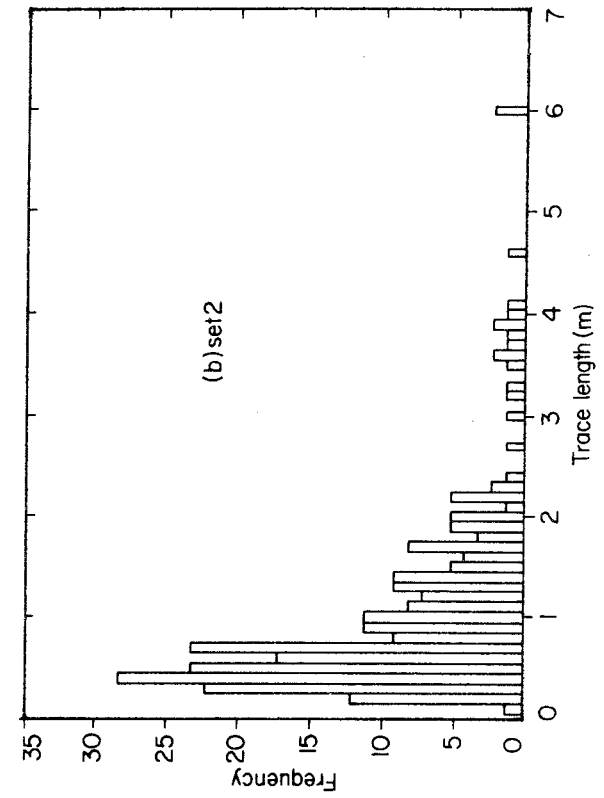

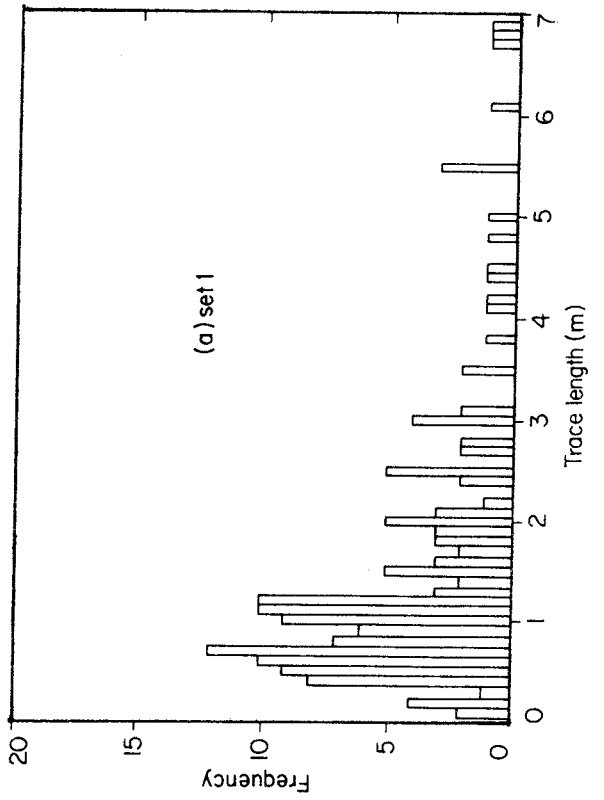

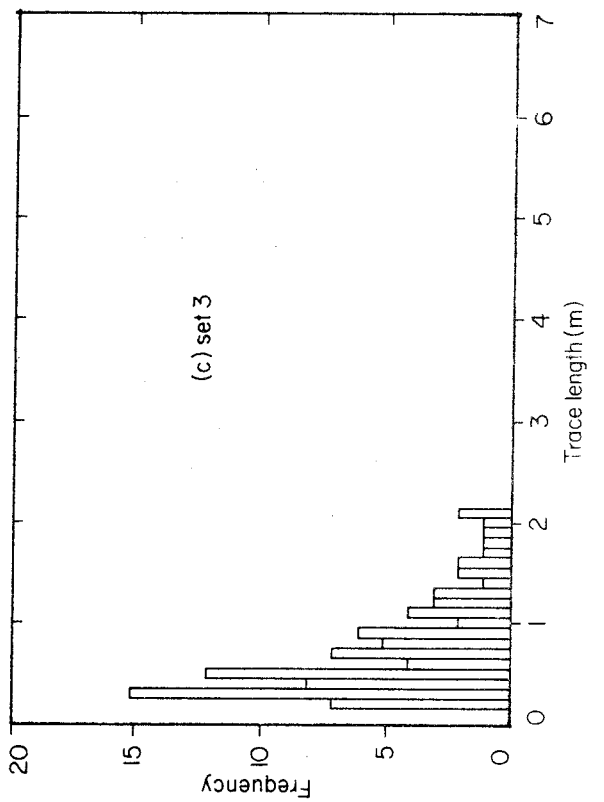

XBL 799-11296

Fig. 16. Fracture length-frequency histograms for the three non-horizontal joint sets [22].

3.5 Aperture

Direct measurement of joint apertures as they appear in boreholes or on exposed blasted rock surfaces is difficult and hardly accurate, particularly since it is basic to rock structure that the aperture of one and the same joint or fracture varies considerably. Actually, stresses in rock due to gravitation and tectonics have to be transferred between adjacent block units, which requires local contact regions also in joints which appear to be open at local inspection. The spacing of such contacts is determined by the bulk strength and creep properties of the units; it can hardly be more than a few meters in open, slot-shaped joints which have persisted over a time period of a few hundred years or more at 500 m depth, provided that the primary stress situation is fairly isotropic. Larger, suitably shaped voids, caves etc. may of course be stable for rather extreme periods of time due to arching.

The only practical means of determining or estimating the aperture is by steady-state injection testing. It yields equivalent "hydraulic" apertures assuming ideally smooth, parallel plate flow. They are somewhat smaller than the actual aperture but still provide a safe basis for the estimation of the joint space. The data from Stripa are presently being prepared for publication by the LBL. Some major features are presented in Table 4[1)].

It is obvious from Table 4 that this particular granite, although rich in joints, contains very few large passages.Even if it is assumed that the theoretical derivation underestimates the aperture by 100% it would still mean that only about 15% of all joints have an aperture larger than 0.2 mm and only about 2.5% of all joints be as wide as 0.2-0.4 mm.

[1)] The data were taken by LBL and kindly put to the author's disposal by Dr. Charles R. Wilson, LBL.

Table 4. Single open rock joint apertures (mm) in Stripa granite as interpreted from 320 m packer-sealed borehole tests (LBL). Total number = 169.

Interval d, mm	Fraction %
$d \leq 0.01$	78.7
$0.01 < d < 0.05$	13.6
$0.05 < d < 0.10$	6.5
$0.10 < d < 0.20$	1.2
$d \geq 0.20$	0

3.6 Rock joint space, "rock porosity"

Experience shows that the porosity of crystalline rock ranges between a small fraction of one percent and about 2%. Various estimations have yielded values which are usually about 0.5-1%. Assuming, for instance, that the frequency and aperture of the joints specified in Table 4 are representative of a rock cylinder with a length of 320 m and a cross section of 0.1 m^2 we would arrive at a porosity of about 0.75%. We can furthermore conclude that the joints wider than 0.05 mm represent only slightly more than 40% of the total voids, while the corresponding figure for joints with an aperture ranging between 0.1 mm and the maximum aperture 0.2 mm is only about 10%. The latter fraction of joints thus represents a rock porosity of about 0.1%. These joints are the ones of interest with respect to clay migration.

3.7 Simplified model

3.7.1 Joints

There is no doubt that the frequency, orientation, aperture, and degree of continuity of joints in rock usually vary to an extent that points to the need of applying stochastic principles in the formulation of adequate physical flow models and their mathematical analogies. Yet, for sufficiently small rock volumes that contain a moderate number of joints which can be identified in boreholes, simpler models can still be used and this applies to the close proximity of deposition holes of the KBS concept type. For the present study we will consider a plate-shaped 100 m^3 block of igneous rock, its base dimensions being 10x10 m and its thickness being 1 m. The hydraulic conductivity k of this block is assumed to be of the order of 10^{-8} - 10^{-9} m/s, which is a reasonable value for the host rock of a real repository. Since wider joints represent the most serious conditions with respect to erosion of clay gels entering the joints, we need to choose a physical model for the system of joints in the block that fulfils not only the "gross permeability" criterion but which is also characterized by reasonable frequencies and apertures of the individual joints. If we apply the average frequency implied by the statistical population of open fractures in Table 4 we find an average spacing of 1.89 m. It is reasonable, however, to assume the more conservative figure 1.0 m. As to the aperture, a Gaussian distribution of the (average) width of the slot-shaped joints can be taken as a basis of the flow rate estimation and a reasonable approach would be to apply the outcome of the discussion in chapter 3.5, i.e. to assume that the widest joints have an average aperture of 0.4 mm. Accepting the somewhat higher figure 0.5 mm and assuming that the most narrow, clearly water-bearing joints have an average aperture of about 0,1 mm, and neglecting furthermore flow-restricting features like limited trace lengths and tortuous cross-linking, the block under considera-

tion can be illustrated as shown in Fig. 17. The 20 joints represent a theoretical pore volume of about 0.2 m^3, which means that the porosity of the block model is about 0.2%. The assumed distribution of apertures is very conservative with respect to the frequency of wide joints as can be concluded from the example of actual distribution in Table 4.

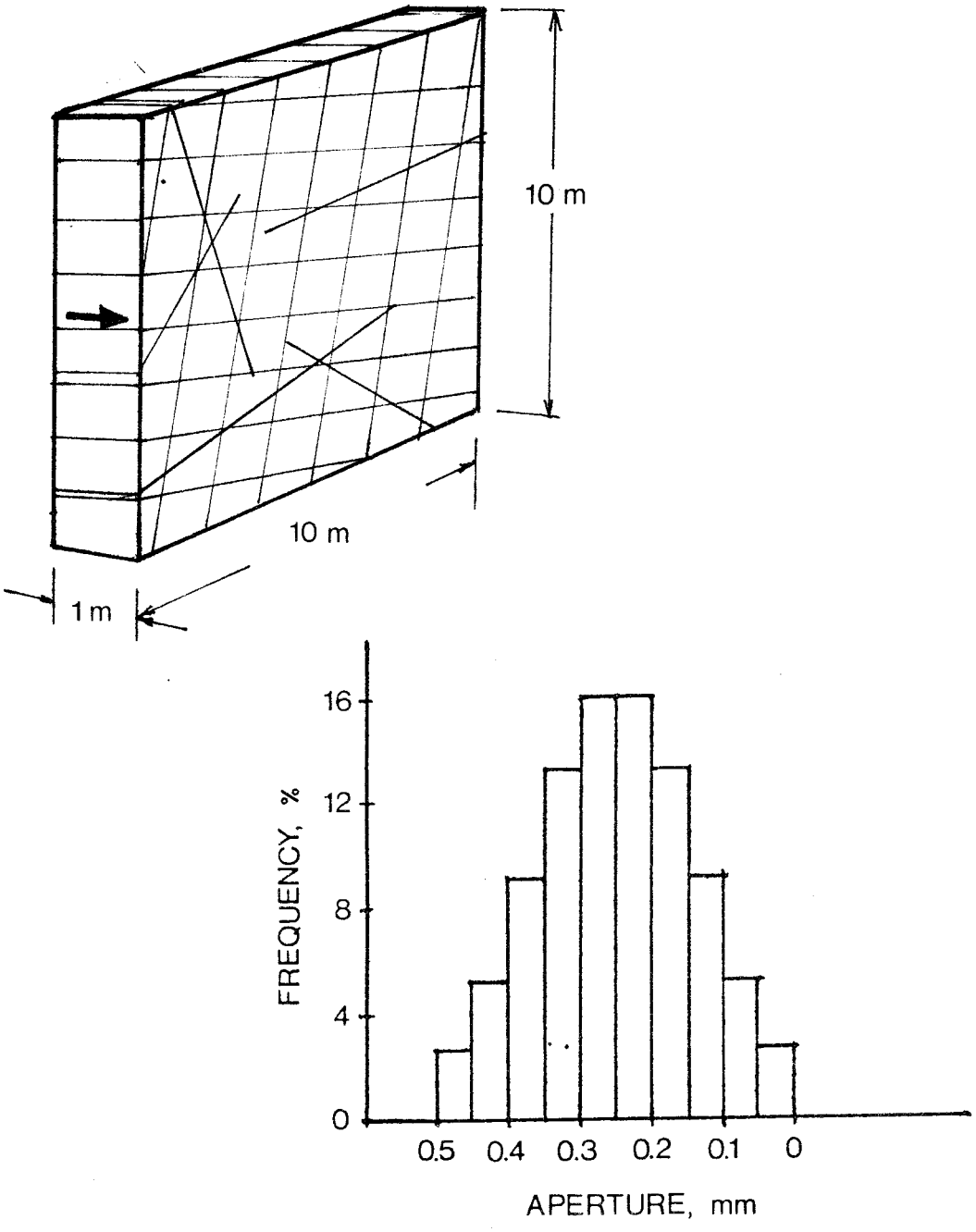

Fig. 17. Upper picture: schematic appearance of block with joints; arrow indicates flow direction. Lower picture illustrates the assumed variation in aperture.

3.7.2 Water flow

The most critical condition with respect to the eroding effect on clay gels from the deposition holes is present in the joints with the widest aperture (0.5 mm). Considering again our block we can estimate the rate of flow through it for the case of unlimited access to water on the high pressure side, meaning that the hydraulic gradient is the same in all the joints. Applying elementary hydraulic relationships for flow in a plane slot, for which the Poiseuille conditions should be reasonably well suited when the rate of flow is very slow, we thus arrive at:

$$v = \frac{d^2 \cdot g \cdot \rho_w}{12\eta} \cdot i \qquad (1)$$

v = flow rate, m/s
d = joint aperture, m
g = gravity, m/s^2
ρ_w = bulk density of water, kg/m^3
η =viscosity of water $\sim 10^{-3}$ Pas
i = hydraulic gradient

This yields an approximate average flow rate of about $0.2 \cdot i$ m/s. After the sealing of the repository, i will approach the regional hydraulic gradient which is of the order of 10^{-3}. At this stage the average flow rate in the widest joints will then be of the order of $2\text{-}4 \cdot 10^{-4}$ m/s, the higher figure referring to the temperature raise in the first few hundred years which lowers the viscosity of the water.

3.7.3 Conditions around a deposition hole

The KBS concept for high level wastes implies full--face drilled deposition holes with a diameter of 1.5 m and a length of about 8 m. Applying our simple model we find that each hole will intersect about 10-15 joints at maximum. If the higher value is used as a basis for further analysis, the joints extending

from the hole will have the individual features given in Table 5. The table also gives the calculated space of each individual joint for an assumed radius of influence, in the plane of the respective joint, and extending from the periphery of the hole, of 3 and 5 m. These figures will be useful in the evaluation of possible bentonite loss.

Table 5. Rock joint features in the near-field of a deposition hole.

Joint aperture mm	Number of joints	Exposed aperture, m^2	Joint space, radius of infl. 3 m m^3	Joint space, radius of infl. 5 m m^3
0.45-0.50	1[1)]	0.0022	0.020	0.048
0.40-0-45	1	0.0020	0.018	0.043
0.35-0.40	2[1)]	0.0017	0.016	0.038
0.30-0.35	2	0.0015	0.014	0.033
0.25-0.30	3[1)]	0.0013	0.012	0.028
0.20-0.25	2	0.0011	0.010	0.023
0.15-0.20	2	0.0008	0.008	0.018
0.10-0.15	2[1)]	0.0006	0.006	0.013
0.05-0.10	1	0.0004	0.004	0.008
0-0.05	1	0.0001	0.001	0.003
			Sum of all joints Σ 0.19 m^3	Sum of all joints Σ 0.44 m^3

1) Numbers adjusted in a conservative way

4. GEL MIGRATION

4.1 Premises

Turning back to our primary object, i.e. that of bentonite migrating into joints which traverse the deposition holes, we now need to specify the physical processes involved in the expansion in order to get a basis for the derivation of relevant physical and mathematical models. Exploratory investigations have shown that the driving mechanism that yields expansion, is the affinity of smectite minerals to water and that the main rate-limiting factor is the aperture of the joint through which the gel propagates, provided that this aperture is smaller than 5 mm [2], [23]; cf. also [24]. These investigations, which were largely empirical and ran for very short periods of time, formed the basis of a theoretical model for "free expansion", i.e. with no influence of Poiseuille-type retardation, which yields penetration rates of a correct order of magnitude when applied to relevant practical geological examples [2]. Since the actual apertures will be smaller than 0.5 mm, according to our rock model, we must here consider the Poiseuille mechanism as well.

4.2 The basic mechanisms

Penetration of clay from the highly compacted bentonite into rock joints requires water percolation through the protruding clay in the opposite direction of propagation in order to keep up the water uptake, which is the driving mechanism. This basic mechanism implies that the rate of penetration is governed by the hydraulic gradient and the permeability. At the beginning of the expansion, the suction, expressed in terms of (negative) pore pressure, is uniform. In the course of swelling the suction drops while the permeability is increased (Fig. 18). The penetration of the clay is retarded by wall "friction" effects which are due to surface roughness as well as to physico/ /chemical interaction between the clay particles and

certain rock-forming minerals.

The derivation of a mathematical model for the expansion and softening rates of clay penetrating into joints, requires formulation of physical models for the basic mechanisms. This implies definition and deduction of the relationships between:

- Suction (u) and bulk density (ρ)
- Permeability (k) and bulk density
- Clay viscosity (η) and bulk density

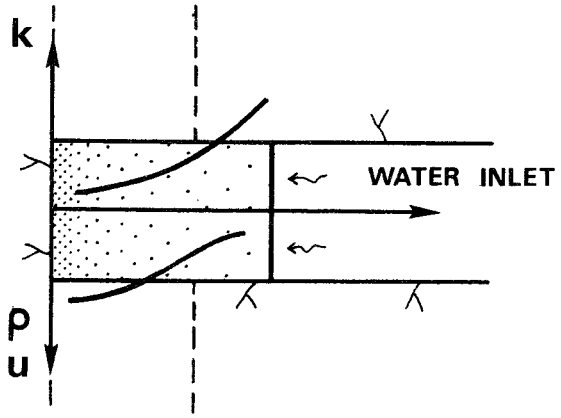

Fig. 18. Schematic picture of "free expansion", i.e. swelling of a dense clay body resulting in a drop in density ρ towards the advancing front. k- and u- changes are discussed in the text.

4.2.1 "Free expansion"

The expansion process can be understood as reversed consolidation, for which several theories have been developed in soil mechanics (cf. [25]), and for which the rheological models shown in Fig. 19 can be taken as representative. These theories imply that the permeability and the relationship between stress and pore volume (or density) be known, and that the initial and ultimate pore water pressures can be defined.

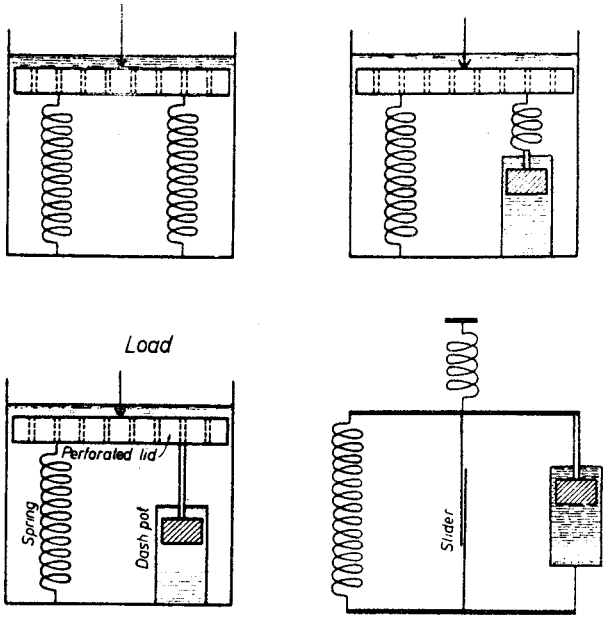

Fig. 19. Basic rheological models for the consolidation process. The perforated lids are flow resistance elements.

These theories are not directly applicable to our present problem since they imply constant permeability and a constant stress/density relationship (or more or less incorrect assumptions concerning the influence of density on these properties). In our expansion case there is a very large density span and, consequently, also variations in permeability and stress/strain properties that cannot be neglected. A reasonably simple and accurate way of estimating the rate of expansion is to perform the calculation in a stepwise fashion as shown in Fig. 20.

The physical model for smectite hydration implies that one and the same pressure is required to expell water as well as to prevent further water uptake of this strongly hydrophilic substance, at least at high bulk densities, cf. [26], [27], [28]. This means that we can derive the "suction" from the available, very comprehensive swelling pressure data [29]. As to the permeability there is a sufficient empirical basis for practical use as well [30]; a reasonable choise of data of both these parameters being collected in Table 6.

Table 6. Approximate permeability (k) and suction [negative pore pressure (u)] for Na bentonite at various bulk densities (ρ_m). (Temperature interval 15-70°).

ρ_m t/m^3	-u MPa	k m/s
1.7	~0.4	$8 \cdot 10^{-14}$-10^{-12}
1.8	0.5-1	$5 \cdot 10^{-14}$-$8 \cdot 10^{-13}$
1.9	2-3	$3 \cdot 10^{-14}$-$5 \cdot 10^{-13}$
2.0	5-10	$2 \cdot 10^{-14}$-$2 \cdot 10^{-13}$
2.1	20-30	$1.5 \cdot 10^{-14}$-$1.5 \cdot 10^{-13}$

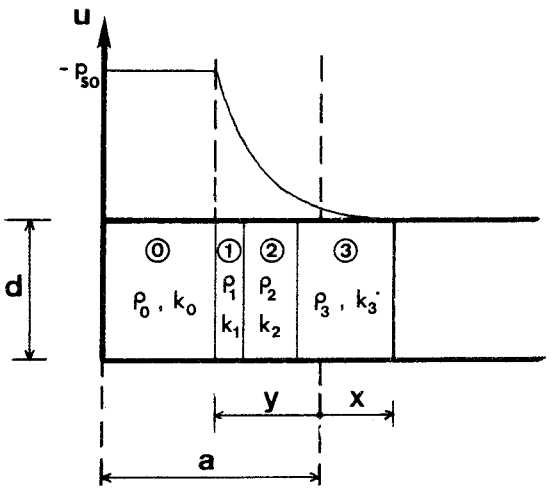

Fig. 20. Model for stepwise calculation of the expansion process in a clay zone with the original density ρ_o, negative pore pressure u_o, and permeability k_o. x represents the expansion of the zone, while y represents a softened part.

For large a-values, covering the case with canisters surrounded by 3-4 decimeter thick annuli of highly compacted bentonite, the time-dependent displacement y of the front is shown in Fig. 21. The main part

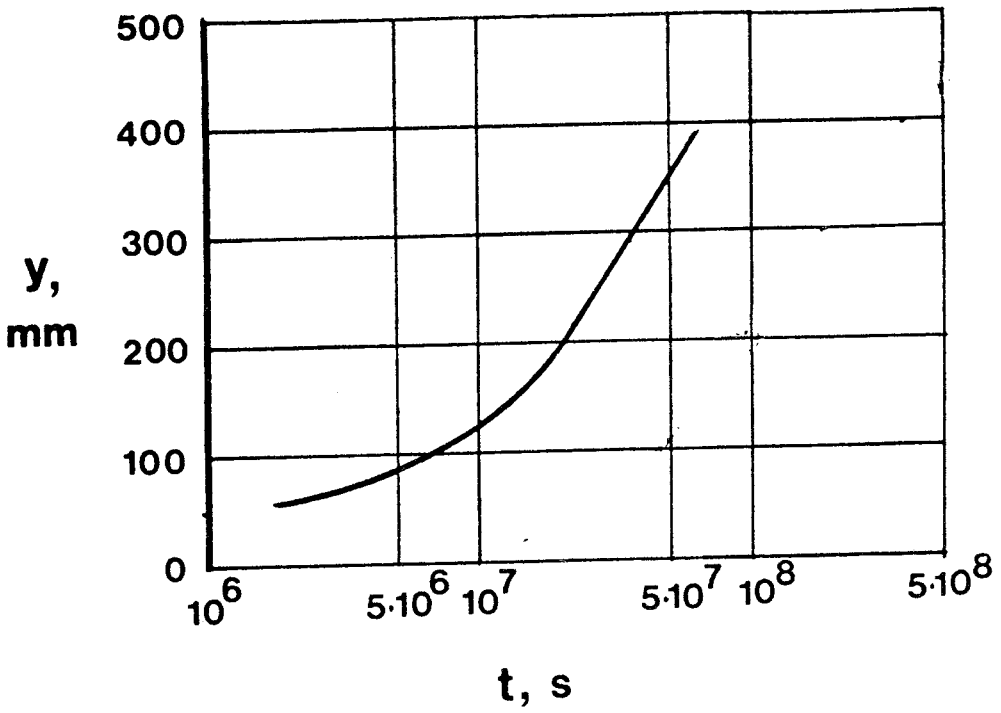

Fig. 21. Displacement (y) of the front of the expanding clay as a function of time (t), [24].

of the protruding gel has an average density of about 1.7 t/m^3 for $t=7\cdot10^7$s (about 2.2 years). For lower densities we know that deviations from the parallel smectite flake organization become obvious. This means that the swelling pressure drops rapidly with decreasing density, while the permeability should be less strongly reduced. At the ultimate, stable density characterized by no swelling pressure, there must still be a slight flow resistance, meaning that the process is more strongly retarded for high t-values than is implied by the log t dependence of the curve in Fig. 21. It is therefore conservative to apply this relationship in correlating the extension of the expanded clay gel and time after the onset of expansion. The correlation is given by Table 7.

Table 7. Displacement (y) of the front of the expanding clay as a function of time (t).

Time t, years	Displacement y, m
10^{-1}	0.07
$10^{0}=1$	0.22
10	0.65
10^{2}	1.08
10^{3}	1.51
10^{4}	1.94
10^{5}	2.37
10^{6}	2.80

Already at this stage we see that even if the Poiseuille effect is omitted, the loss of bentonite through joints which traverse deposition holes will be very small. Thus, by using Table 5 we see that our rock model predicts that only about 0.19 m^3 bentonite will have entered the system of joints in 10^6 years. Making the very conservative assumption that this bentonite has the same bulk density as the highly compacted bentonite in the deposition holes, i.e. about 2.1 t/m^3, we arrive at the conclusion that only 0.19 m^3 out of about 10 m^3, i.e. about 2%, will be lost. This loss is of no practical importance and we therefore do not need to improve the calculation. However, there is definitely a positive effect of bentonite entering the joints to a moderate depth, since it will help to retard groundwater percolation and diffusion of ions to and from the canisters. It is therefore still of interest to refine the model so that it can be definitely decided whether the clay filling will even be beneficial. This brings us back to the simple "free expansion" model which must now be combined with a retarding component to account for the Poiseuille effect.

4.2.2 The "Poiseuille", extrusion case

The retarding effect of interaction between the expanding clay and the rock exposed in the joints can be considered by applying flow theory. For this purpose we need to know the viscosity as a function of the density of water saturated bentonite. There is a very limited number of systematic determinations of this quantity but recent viscometer studies, reported in a subsequent chapter, creep tests, as well as a literature survey has led to the rough estimates in Table 8. It indicates that the viscosity is very low when the density drops below about 1.3 t/m^3, which indicates that the main rate-determining effect appears in the upper density range.

Table 8. Approximate viscosity values for bentonites

Density, ρ_m t/m^3	Viscosity, η MPas	Source
1.9	10^6-10^8	Author's current creep tests;
1.5	10-10^4	Literature data
1.2	$2 \cdot 10^{-2}$	Author's viscometer tests
1.1	$\sim 10^{-4}$	"-

In this context the upper end of the viscosity range for each density represents the most conservative case. These values fit an exponential expression of the type:

$$\eta = e^{20(\rho_m - 1)} \qquad (2)$$

which will be used as a first approach in the subsequent analysis: η is expressed in MPas when ρ_m is in t/m^3 ($\rho_m > 1.2$ t/m^3).

A very simple model, analoguous to that of free swelling, has been used to illustrate the order of magnitude of the viscous rate effect (Fig. 22).

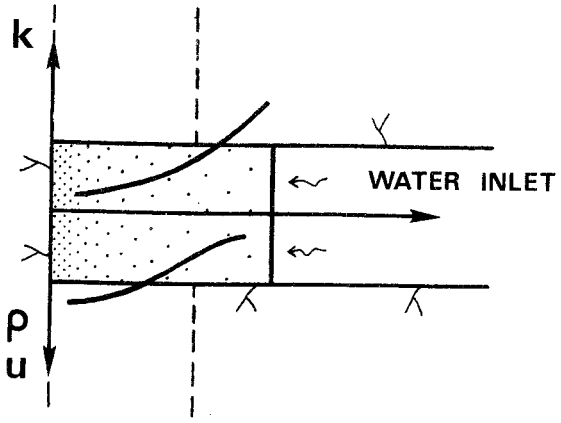

Fig. 22. Schematic picture of the viscous flow model.

The driving force is the difference in swelling pressure, which drops successively in the direction of flow due to the expansion through water uptake. Applying again Eq. (1)* and using the symbols:

$$i = \frac{\partial p_s}{\partial x}$$

v = average extrusion rate

d = aperture

p_s = swelling pressure

η = clay viscosity

we are thus able to calculate the extrusion rate. The application of this flow law requires, however, that the viscosity is uniform and that the gradient is constant. Since these criteria are not fulfilled, it is called for a step-wise approach as in the case of free expansion. The first step is schematically shown in Fig. 23. The swelling pressure, which is directly derived from Table 6, i.e. the positive equivalent of the suction, drops rapidly when the density is reduced, but since there is an even more drastic drop in viscosity on expansion it is concluded that the major influence of aperture on the migration rate is in the initial phase of penetration. A very simple check illustrates that this approach is actually a determi-

*simplified form

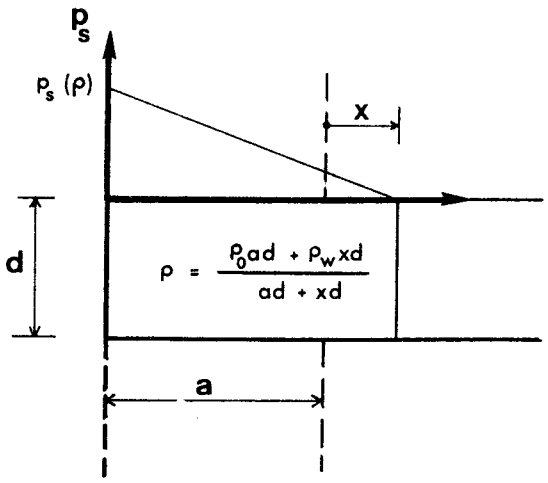

Fig. 23. Simplified model of clay extrusion considered as a viscous flow process.

nant of the penetration rate. Thus, we find by considering the early stage with x=1 mm for d=0.1 mm that whatever reasonable a-value that is applied, the time required for an additional 1 mm penetration is at least several months. This is very much slower than the free expansion rate, which thus illustrates the importance of the aperture.

The very slow penetration rate caused by the flow resistance in narrow joints means that there is sufficient time for the remaining mass of highly compacted bentonite in the deposition holes to maintain a highly homogeneous state through internal mass flow and creep. The density and therefore also the swelling pressure at the inner end of the joints can therefore be taken as a constant and since the penetration will have a negligible effect on the density of the bentonite in the holes, it will remain to be about 2.0 t/m^3 which corresponds to a swelling pressure of about 8 MPa. As a rough approximation we can therefore estimate the penetration rate by applying the model in Fig. 23 with a=0. The density of the protruding clay will be assumed to vary linearly from 2.0 t/m^3 at the inner end (x=0) to 1.5 t/m^3 in the outer part of the clay,

thus disregarding the possible existence of a soft clay gel at the very front. Hence, we will consider the extrusion of a clay film with a constant average density of 1.75 t/m^3, and an assumed viscosity of $10^{6.5}$ MPas. The extrusion rate drops in the course of the penetration since the pressure gradient will be reduced as a consequence of the displacement of the clay front. Applying stepwise calculation we find that this displacement can reasonably well be described by a log t law of the following empirical form:

$$x = A \cdot d^2 \log(t+1) \qquad (3)$$

where x = displacement of the film front
d = aperture
t = time after the onset of flow (t>0)
A = constant

For x and d in meters and t in years, A will be approximately $5 \cdot 10^4 - 10^6$, the lower value corresponding to the upper viscosity range. This value thus represents the most conservative case; it yields the approximate extrusions given in Table 9.

It is concluded that clay films with a considerable density will enter joints with an aperture of about 0.1 mm or more. With the presently applied, very conservative scenario, the rate of filling will obviously be extremely slow in the joints of our rock model, which suggests that the rock-sealing ability is very small in the first few million years. However, a realistic analysis requires that temperature be taken into consideration as well, which alters the picture considerably. Thus, experience as well as theory shows that a temperature rise from about 15 ^{o}C,

Table 9. Estimated extrusion in meters of clay in rock joints. Average density 1.75 t/m^3.

Joint aperture, mm	t=2y	10y	10^2y	10^3y	10^4y	10^5y	10^6y
0.1	$1.5\cdot10^{-4}$	$5.2\cdot10^{-4}$	10^{-3}	$1.5\cdot10^{-3}$	$2\cdot10^{-3}$	$2.5\cdot10^{-3}$	$3\cdot10^{-3}$
0.2	$6\cdot10^{-4}$	$2\cdot10^{-3}$	$4\cdot10^{-3}$	$6\cdot10^{-3}$	$8\cdot10^{-3}$	10^{-2}	$1.2\cdot10^{-2}$
0.3	$1.4\cdot10^{-3}$	$4.7\cdot10^{-3}$	$9\cdot10^{-3}$	$1.4\cdot10^{-2}$	$1.8\cdot10^{-2}$	$2.3\cdot10^{-2}$	$2.7\cdot10^{-2}$
0.4	$2.4\cdot10^{-3}$	$8.3\cdot10^{-3}$	$1.6\cdot10^{-2}$	$2.4\cdot10^{-2}$	$3.2\cdot10^{-2}$	$4\cdot10^{-2}$	$4.8\cdot10^{-2}$
0.5	$3.7\cdot10^{-3}$	$1.3\cdot10^{-2}$	$2.5\cdot10^{-2}$	$3.8\cdot10^{-2}$	$5\cdot10^{-2}$	$6.3\cdot10^{-2}$	$7.5\cdot10^{-2}$
1.0	$1.5\cdot10^{-2}$	$5.2\cdot10^{-2}$	10^{-1}	$1.5\cdot10^{-1}$	$2\cdot10^{-1}$	$2.5\cdot10^{-1}$	$3\cdot10^{-1}$

which will be the average initial rock temperature, to the 60-80 ^{o}C interval that is expected to last for several hundred years in the vicinity of the deposition holes, will reduce the viscosity. Earlier investigators [31] stated that the viscosity of remolded clay pastes follows the moderate temperature dependence of water viscosity which yields a reduction to 1/4 on raising the temperature from 15-80 ^{o}C. However, temperature is known to be a determinant of the strain rate at high shear stress levels for structurally intact clays, such as the bentonite on entering rock joints [32]. If we also consider the viscosity span in Table 8, much higher extrusion rates can be expected and it is probable that all joints in our rock model will be filled by clay films with an average density of 1.5 t/m^3 or more to within at least 0.1 m from the deposition holes after a few hundred years. For joints with apertures wider than 0.3 mm the filling will probably have an extension of 0.2 m. It is clear, however, that the flow resistance at the clay penetration is a determinant of the clay migration rate and the previous estimation that 0.2 m^3 of dense bentonite will leave each deposition hole in 10^6 years is therefore an exaggeration.

Field observations in natural bentonite deposits show that clay has penetrated far into fractures in adjacent rock [33], but since the time-dependence of such

processes are not known they are of limited interest in the present context.

4.3 Experimental

4.3.1 Pilot tests

Several series of experiments have been run to examine the penetration rate of Na bentonite[1] into artificial joints. Pilot studies have been made by use of a rigid stainless steel cell consisting of a number of discs with notches of various depth so as to simulate joints with the apertures 0.5, 0.3, 0.15, 0.10 and 0.05 mm, through which water was allowed to enter and through which the swelling bentonite could penetrate (Fig. 24). The bentonite was compacted in the cylindrical cell to a bulk density of about 2.1 t/m^3 and a water content of about 10%, which corresponds to a degree of water saturation of about 50% and which is expected to yield a bulk density of slightly more than 2.2 t/m^3 after water saturation. The sample was confined in the cell so that no expansion could take place except for the swelling and extrusion through the slots. The penetration of bentonite was determined at various time intervals by means of thin metal blade sensors which were pushed through the slots. The main outcome of these test series was the observation that bentonite actually entered the slots and that it formed a fairly stiff mass, which is in agreement with our premises in the application of the viscous flow model. Also in agreement with theory was the observation of a narrow, very soft gel-type region at the front (Fig. 25). This region appeared to be separated from the stiffer gel film by a clear boundary [23]. The first test series, which was made with $3 \cdot 10^{-2}$ M NaCl solution, ran for only about 2 months and showed

[1] The standard KBS reference Na bentonite, MX-80 (American Colloid Co.) was used in the author's tests.

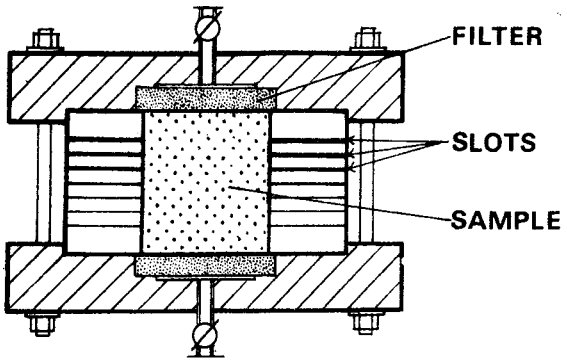

Fig. 24. Cell for determination of bentonite penetration in narrow slots. The sample diameter is 50 mm.

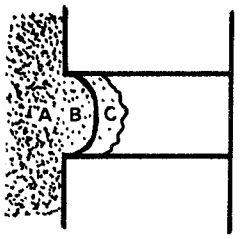

Fig. 25. Schematic picture of observed zones in wider slots. A very stiff bentonite, B fairly stiff region, C very soft region.

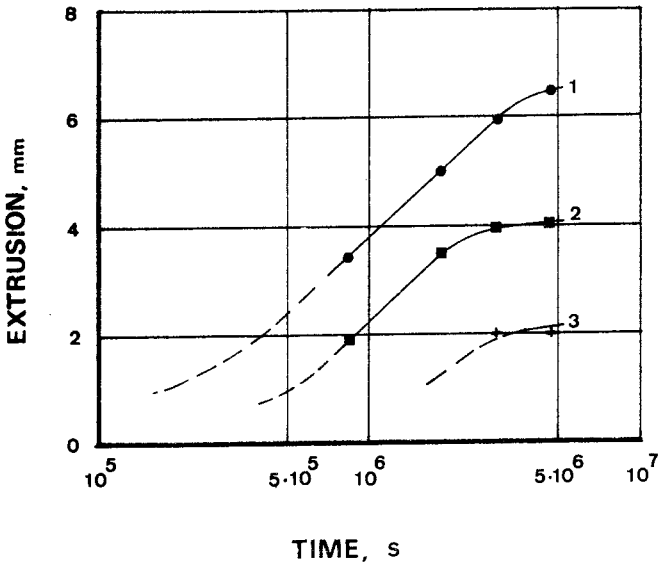

Fig. 26. Measured penetration of "stiff" bentonite into slots formed by metal discs.

that the front of the stiffer clay film had moved about 6.5 mm in the slot with 0.5 mm aperture in this period of time. The corresponding distance was 4 mm in the slot with 0.3 mm aperture, and about 2 mm in the 0.15 mm slot, while no bentonite had entered the 0.1 and 0.05 mm slots. The penetration rate appeared to drop with time according to a log t law, and seemed to be further retarded at the end of the observation period, cf. Fig. 26.

A second pilot series was run for 40 days with a concentrated NaCl solution (0.6 M), and distilled water to get a check on the influence of the groundwater salinity. The bulk density of the bentonite core was a little lower than in the first series, the water content now being in the range of 26-29%, which corresponds to the bulk density interval 1.95-2.0 t/m^3. This investigation showed that the front of the stiffer clay had moved 5 mm in the 0.5 mm slot in the salt water and 8 mm in distilled water. The corresponding distances in the 0.3 mm slot were 3 and 5 mm, respectively, while they were 1.5 and 3 mm in the 0.15 mm slot. In distilled water there was even a tendency for bentonite to enter the 0.1 mm slot.

It is concluded that the salinity of the water has some, relatively minor influence on the penetration rate – which is in agreement with the expected change in swelling pressure when the density drops below 2 t/m^3 [29] – and that the observed rates are much higher than the predicted ones according to Table 9, which therefore offers over-conservative estimates.

4.3.2 Main test series

Equipment

The various modes of interaction between the clay gel entering a joint in crystalline rock and its crystal matrix called for a series of long term tests using granite blocks rather than steel cells. Overcored borehole blocks of granite with an outer diameter of 142 mm had been split in a previous study of borehole sealing and were rearranged and glued together to form discs with a central hole diameter of 39 mm and a height of about 50 mm for the present experiment. Their basal surfaces were ground to become plane and pairs of blocks were then anchored together with the plane surfaces facing each other to form well defined artificial joints. Their aperture was controlled by a few radially oriented thin metal blades of non-corrosive material (Fig. 27). The granite discs were centered and locked in position between metal plates, their outer ends being separated from the metal by 2 mm rubber discs to offer a uniform external support and to avoid axial leakage of expanding bentonite from the hole in which tightly fitting precompacted cylinders of MX-80 bentonite were inserted. The metal plates were equipped with central, large bolts (cf. Fig. 27) which served to keep the bentonite core axially confined during testing. The arrangement thus gave similar conditions as those in a deposition hole in the sense that saturation took place by water uptake through the slot into which clay could migrate at the same time.

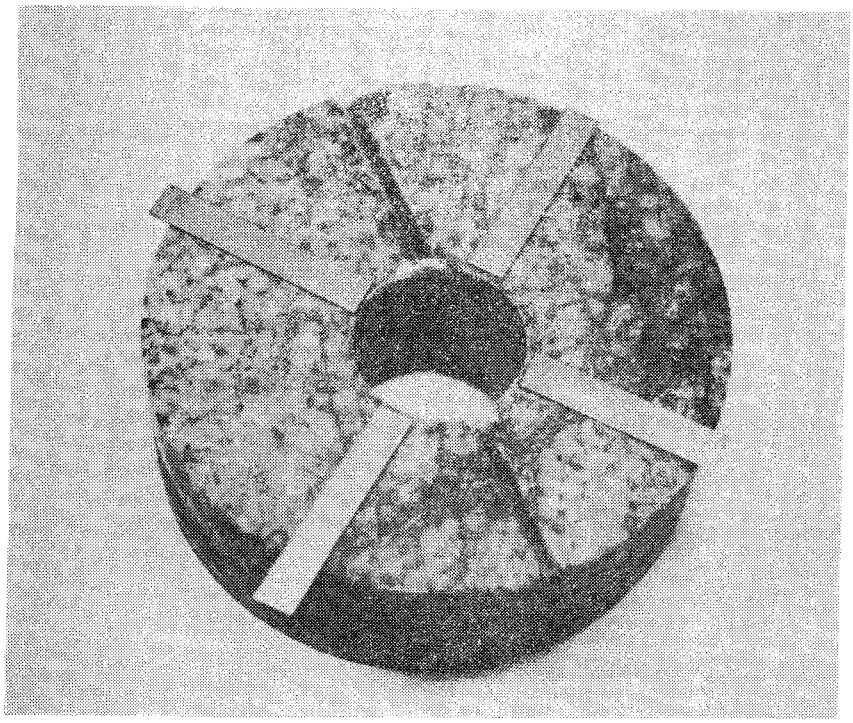

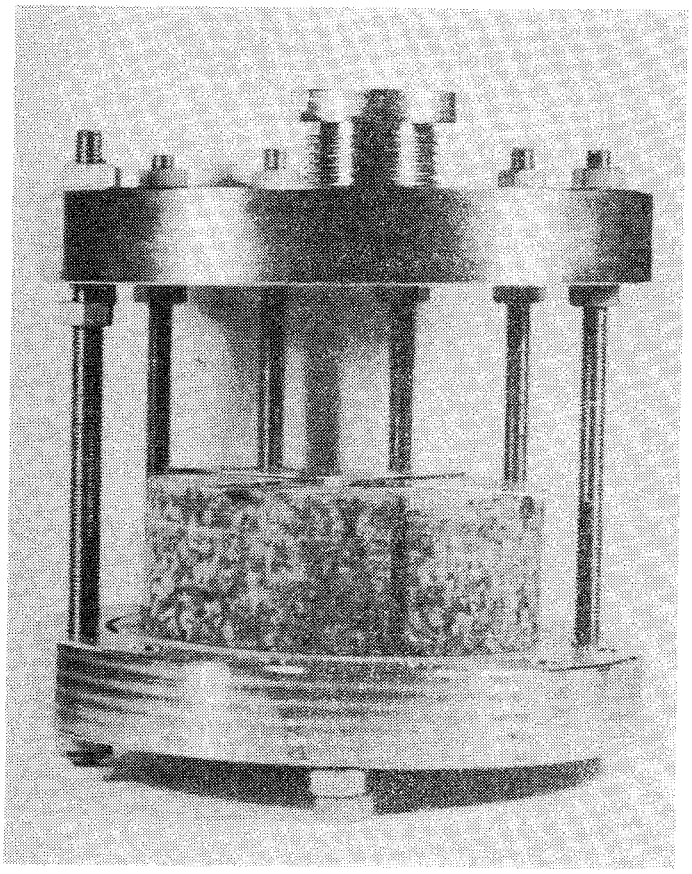

Fig. 27. Granite discs for slot tests. Upper picture shows glued halves forming one disc. Lower picture shows the cell for anchoring the two discs; the lower disc being in position.

The bentonite, which had an initial water content of 6% was compacted to a bulk density of 1.8 t/m^3. This would yield a water content of 34% and a bulk density of about 1.9 t/m^3 at complete saturation. At the end of the tests, which lasted for 2-3.5 months, careful sampling was made to determine the water content of the clay core in the holes. It turned out to be very uniform and showed that practically complete water saturation had taken place throughout the cores even in the case of a slot with only 0.1 mm aperture (cf. Fig. 28). The pressure, which was required to extrude the cores, was correspondingly uniform and gave the "bond strength" value of about 250 kPa for all samples.

Arrangements were made to identify the successive penetration of bentonite into the slots. For this purpose a groove was cut in the acrylate plastic, which combined the semi-circular granite bodies, so that the lense of a fiber optics system could be inserted for inspection. The groove was isolated from the slot by a rigid transparent glass cover as shown in Fig. 29. The device for anchoring the granite discs together is seen in Fig. 30, which also shows the arrangement of the fiber optics system for regular inspection of the submerged samples. Photographs were taken at regular intervals for documentation purposes.

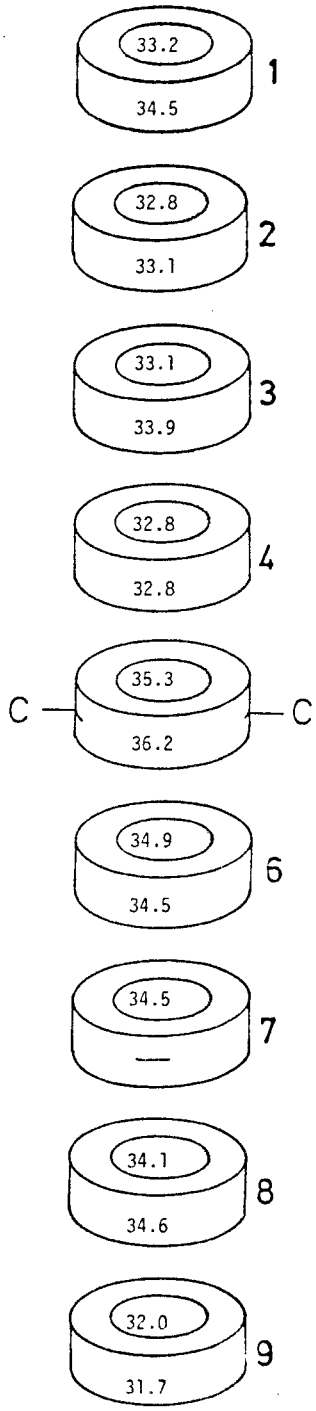

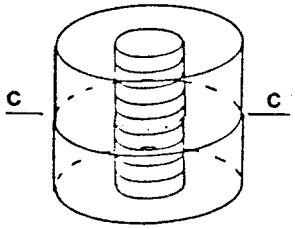

Fig. 28. Water content distribution in split core of 10 cm length after the end of the 0.1 mm slot (c) test (3.5 months). Each disc was cut into a cylindrical nucleus and an outer annulus, both of approximately the same weight. The figures represent the water contents.

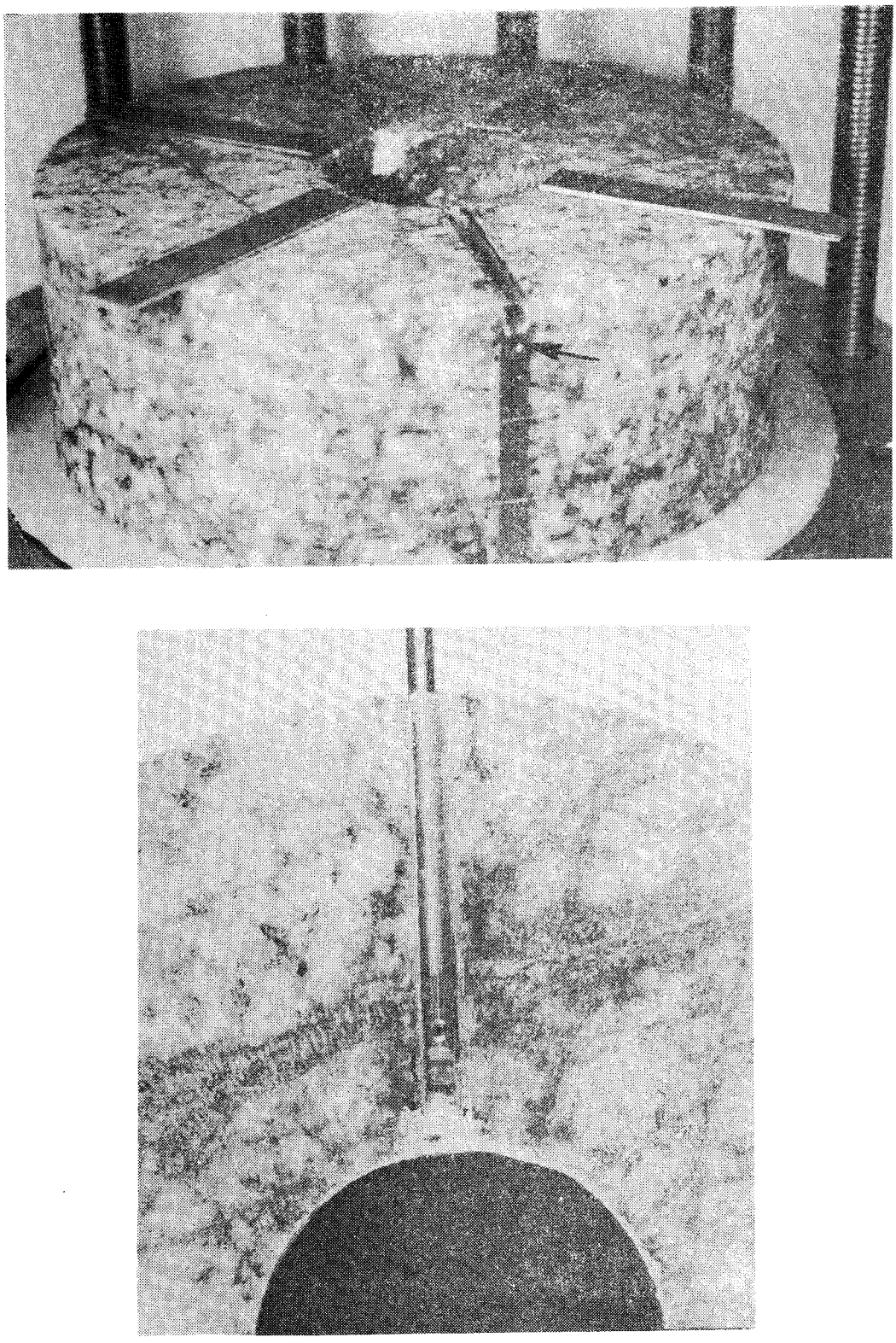

Fig. 29. "Tunnel" (arrow in the upper picture) for insertion of fiber optics close to the slot. Lower picture shows the inserted lense system, the "eye" pointing upwards, towards the "joint", which is formed when the upper granite disc is put in position.

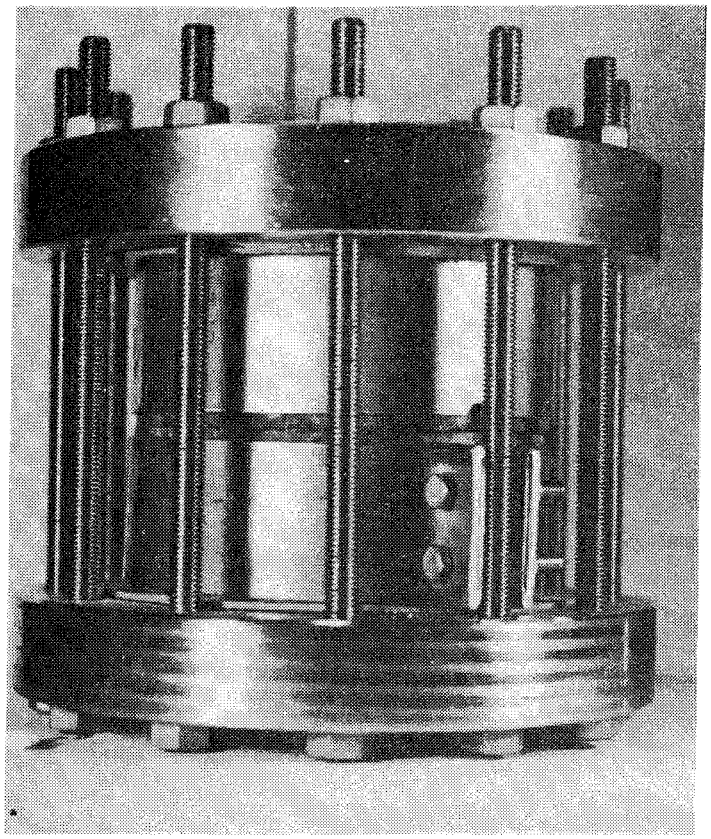

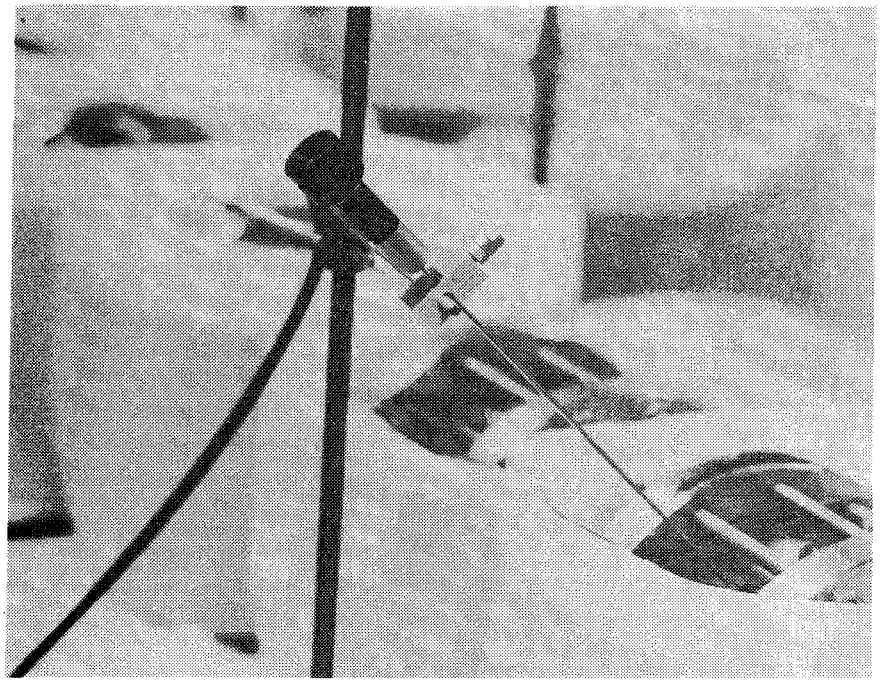

Fig. 30. The test device. Lower picture shows submerged device with fiber optics in position for inspection.

Test program

Table 10 summarizes the test program which originally covered a complete set of experiments with synthetic groundwater ("Allard" water) as well. Only one test, which is still being run (No. 7), was prepared with this type of water, however.

Table 10. Specification of experiments for determination of bentonite penetration into rock joints.

Test No.	Aperture mm	Water	Time days
1	1.0	Aqua dest.	60
2	0.5	"	105
3	0.4	"	105
4	0.3	"	105
5	0.2	"	105
6	0.1	"	105
7	1.0	"Allard"	Running, 105 days at present

Results

The inspection of the bentonite penetration in the slots confirmed earlier observations that the clay film has a soft front part and a stiffer consistency closer to the core. It was also observed that there was a rather distinct boundary between the soft front and the distilled water, which shows that flocculation had taken place. The boundary between the stiffer and softer parts of the clay film was not very clear, however.

The lense of the rod that contains the fiber bundle was situated a few millimeters from its tip and since there was also a sealing at the inner end of the inspection "tunnel", the bentonite front had to migrate 8-10 mm before it could be detected. There was therefore no sign of bentonite in the most narrow

slots until the termination of the test. Fig. 31 shows representative photographs taken by use of the fiber optics system. The upper figure shows the distinct outer boundary of the expanding soft gel in distilled water, which is more homogeneous than the corresponding front part of the gel in "Allard" water.

The exposure of the slots at the end of the tests showed a stiffer, inner part of the clay film and a softer outer part. This pattern is illustrated by Figs. 32-34. The outer contour is very irregular and isolated areas (z) of soft gels are rather frequent. This was caused by the separation of the rock discs at which part of the clay film adhered to one of the rock surfaces, while the remaining parts were stuck to the opposite surface. The average extension of the two zones is given by Table 11, in which also the average densities and water contents are given. The minute quantities of film material did not allow for separate determinations of the water content of the stiffer and softer zones, and should only be taken as a very approximate measure of the consistency of the entire sampled clay film in the slot. A rough estimate yields an average density of the stiff zones of 1.5-1.7 t/m^3.

Table 11. Penetration depth of bentonite.

Test no	Aperture	Av.pen.depth of stiff zone,	Av.pen.depth of soft front	ρ_m [1]	w [1]	Comments
	mm	m	m	t/m^3	%	
1	1.0	0.010	0.030	1.26	198	Aqua dest in test no 1-6
2	0.5	0.007	0.015	1.14	421	
3	0.4	0.005	0.010-0.015	1.15	374	
4	0.3	0.004	~0.01	1.24	231	
5	0.2	0.003	~0.01	-	-	
6	0.1	0.002	~0.01	-	-	
Joint [2]	1.5	0.023		1.39	123	
7	1.0		~0.02			"Allard" water; fiber optics

[1] Average of stiff and soft zones

[2] Refers to test no 6 (105 days)

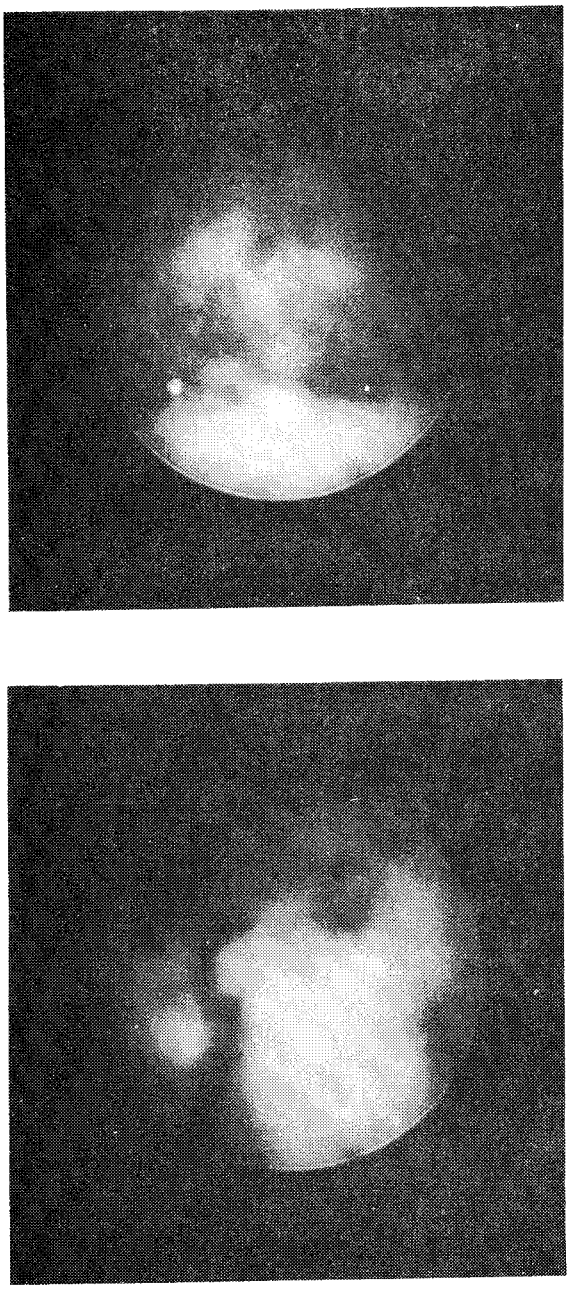

Fig. 31. Micrographs showing the outer boundary of expanding soft gels. The light areas at the lower end is the clay gel which is expanding upwards in the picture. The irregular, greyish area in the upper part is the granite surface.

Upper picture: Distilled water, slot width 0.4 mm. Lower picture: "Allard" water, slot width 1 mm.

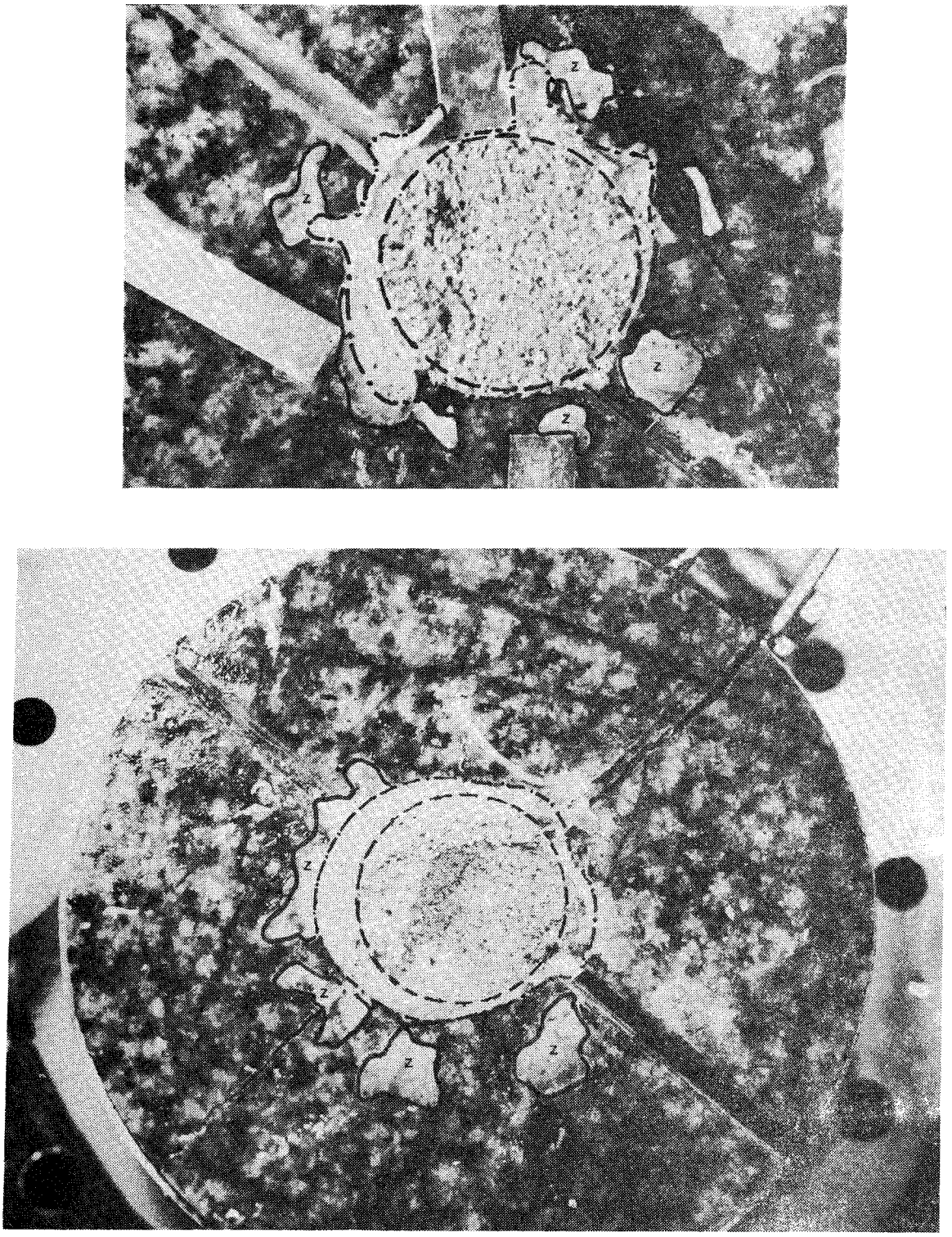

Fig. 32. The exposed clay film.
Contours of original core (- - - -),
outer boundary of stiff zone (- . - . -),
and outer boundary of soft gel (———).
Upper picture 0.5 mm slot; Lower picture
0.4 mm slot. Distilled water.

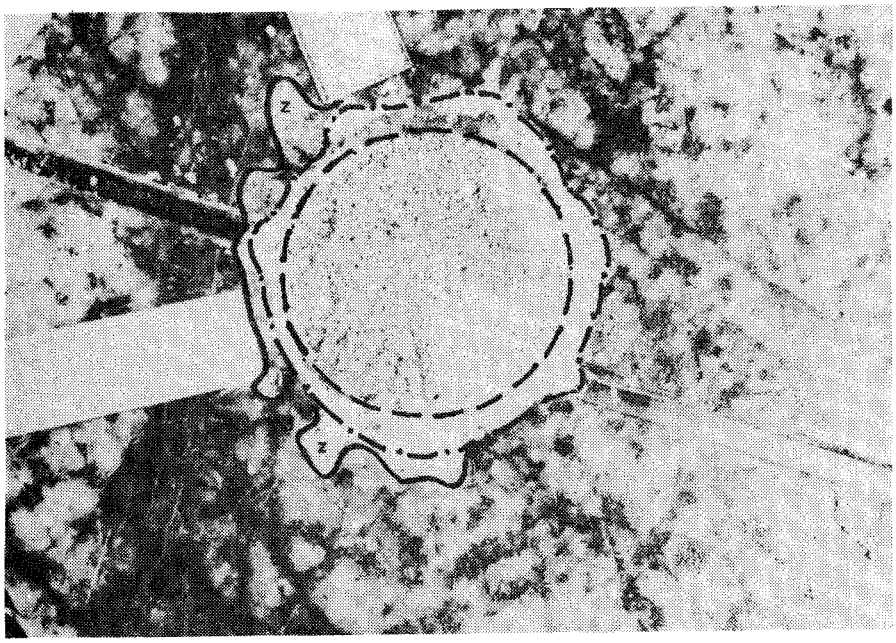

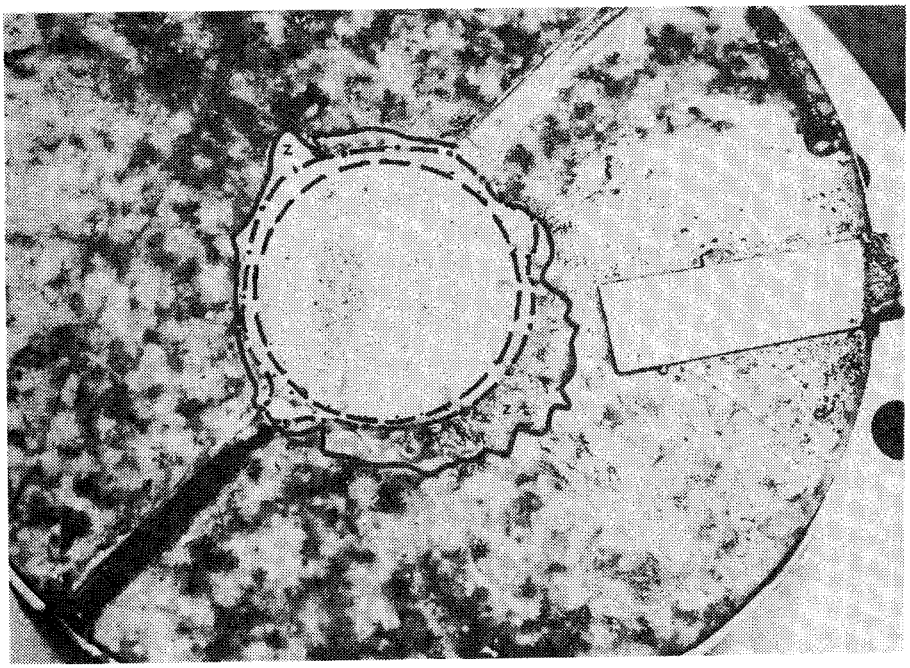

Fig. 33. The exposed clay film (legend in in Fig. 32). Upper picture 0.3 mm slot; Lower picture 0.2 mm slot. Distilled water.

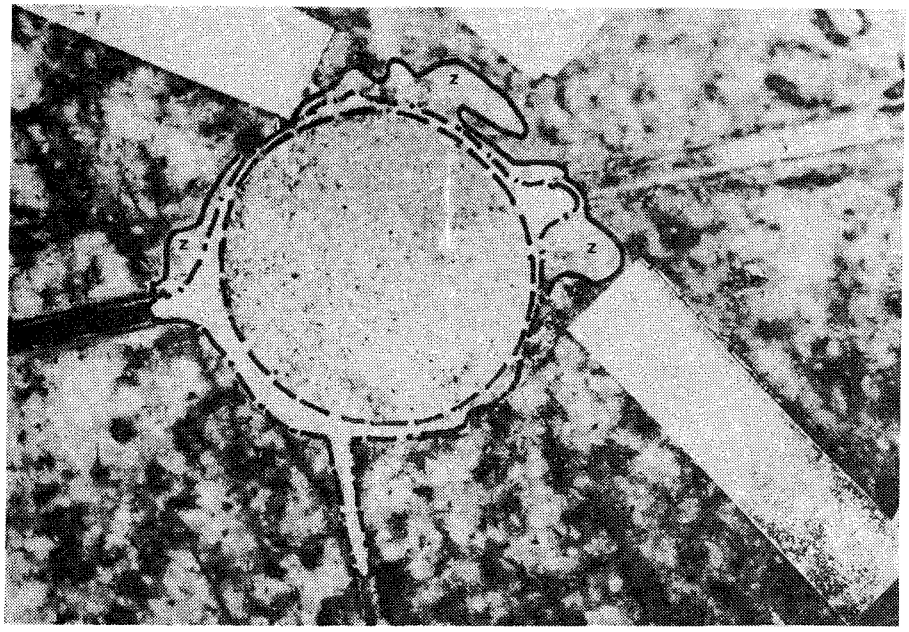

Fig. 34. The exposed clay film (legend in Fig. 32). 0.1 mm slot. Distilled water.

4.4 Conclusions

The experiments all show that the rate of clay penetration into rock joints is much higher than that predicted by the theoretical "Poiseuille"-type model, except for the joints with apertures equal to or smaller than 0.1 mm, which points to a rather strong interaction between the penetrating clay and the crystal matrix only in very narrow joints.

This is supported by the observation that the clay penetration in the granite-disc tests were very much the same as those measured in the wider apertures of the steel device where interactions between the clay and the smooth non-corrosive metal must have been negligible. "Free expansion" is therefore the dominant process which is only relatively slightly retarded in the joints of the presently applied rock model.

The general agreement between the observations from the experiments with the steel cells and the granite-disc device suggests that the log t-dependence of the penetration rate specified by Eq. (3) is valid. However, the observations also show that the penetration rate is much higher than this equation specifies, and support the idea that joints with apertures exceeding 0.1 mm which traverse the deposition holes will be filled with rather stiff bentonite clay to within at least 0.1 m from the holes in a few hundred years. This clay, the density of which is expected to be 1.5 t/m^3 as an average, serves as a valuable sealing of the joints provided that it resists the erosion that may arise from the slow groundwater flow that will take place. This matter is looked into in the subsequent text.

5. EROSION

5.1 Physical aspects

Dispersion, slaking and internal erosion of clays have been well documented in the field of applied soil mechanics and certain specifications for filter design and construction practices are in current use. The susceptibility of a clay to internal erosion increases with its tendency to disperse spontaneously in water or under the drag force of seepage. Direct tests of dispersiveness have been developed, the pinhole dispersion test being particularly valuable since it implies percolation of the soil with water. In this type of test a small soil specimen is compacted at its plastic limit into a permeameter cell. A ϕ 1 mm pin is then pushed through the clay to form a passage for water. After withdrawing the pin and sealing the cell, water is allowed to pass horizontally through the hole under pressure. The flow rate under various heads and the nature of the discharge provide a measurement of erosiveness, by which the soil can be categorized according to a classification scheme. The most dispersive category ("D1") represents soil that fails rapidly under 50 mm head (aqua dest).

Dispersion of expansive clays is known to be largely affected by the so-called sodium adsorption ratio (SAR) which is defined as $SAR=Na/(\sqrt{\frac{Ca+Mg}{2}})$ where the chemical symbols represent the respective amount of adsorbed cation. The dispersibility of such clays is also related to the ESP=(Na/total exchange capacity)x x 100 where the exchange capacity is expressed in milliequivalents per 100 g dry clay. Very low SAR and ESP values (<5) are typical of non-dispersive clays, while higher values than 15 characteristically point to strong slaking. Experience from pinhole tests shows that clays tested with sodium ions occupying more than about 10 percent of the exchange complex exhibit dispersion provided the electrolyte concentration of the fluid is lower than 10^{-3}N. This suggests that the Na-

-bentonite clay that propagates through the rock joints should be very sensitive to erosion. Unfortunately, quantitative estimates cannot be founded on dam erosion experience, since the flow velocity is very much higher than those expected in rock joints. For the present purpose we therefore need to deepen the analysis with respect to the drag forces exerted by flowing water and the counteracting, cohesive interparticle forces.

5.2 Particle bond strength

5.2.1 Introduction

While theoretical considerations do not offer reliable bond strength values (cf. 2.4.2 and 2.4.3), there are various practical ways to estimate the average shear strength of such dilute gels so that the average bond strength can be reasonably well estimated. Such an approach was made by NICKEL who considered clay slurry systems to exhibit flow characteristics which can be defined as quasi-plastic, and who regarded such systems as Bingham plastic fluids [34]. He suggested the use of rotational viscometers for a closer analysis of the erosiveness in terms of the so-called Bingham yield stress τ_B (Fig. 35). It is evaluated as the point where the straight-line portion of the curve is extrapolated to meet the line of zero velocity gradient and correponds physically to the state where particle association or bonding is largely broken down under shear. τ_0 in the figure is a critical shear stress at which flow is just initiated.

This idea was adopted by YONG et al. [35] who illustrated the very obvious influence of pore water electrolytes on the shear resistance of dilute clays (Fig. 35).

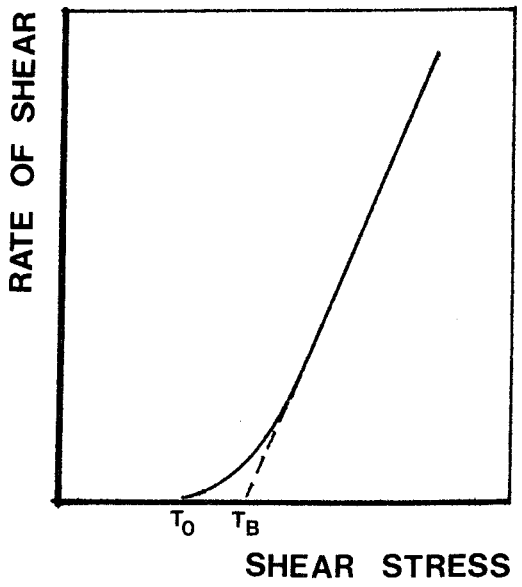

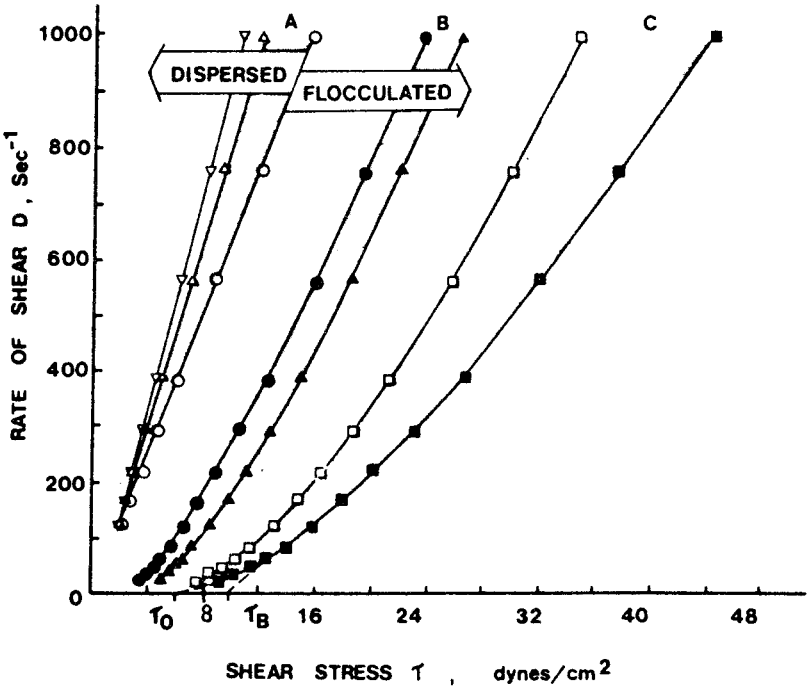

Fig. 35. Upper picture: Relationship between shear stress and rate of shear for a Bingham system.

Lower picture: "Rheograms" of sodium kaolinite with a clay concentration of 9.1% dispersed in various concentrations of NaCl, and 4.9% concentration dispersed in $NaHCO_3$. A is 10^{-5}-10^{-3} M NaCl solution (dispersed); B is $3 \cdot 10^{-3}$-$3 \cdot 10^{-1}$ M NaCl (flocculated); C is 1-3 M NaCl (highly flocculated); ▽ 10^{-2} M $NaHCO_3$ [35].

NICKEL compared his recorded τ_0 and τ_B-values with the shear stress required to produce failure (substantial erosion) in the pinhole test and was able to explain the distinction between dispersive and non-dispersive soils in a qualitative manner. He calculated the shear stress at failure in the pinhole test from:

$$\tau_f = \frac{f \cdot \rho \cdot v^2}{8} \qquad (4)$$

where ρ = fluid density in kg/m^3
f = function of Reynolds number
v = flow rate in m/s
τ_f = shear stress in N/m^2

Eq. (4) refers to turbulent flow in which f depends on the rawness of the "pipe", i.e. the clay surface. Since the rawness is actually not known, NICKEL's expression is of limited value. The only unanimous application of the pinhole test in the author's mind is to use it as an experimental check of theoretical calculations of the balance between water drag forces acting on individual particles and particle bonds that anchor them to the intact gel. As will be shown later in this report it serves well in this respect.

5.2.2 Viscometer tests

Equipment and test procedure

A Swedish BOHLIN Viskosimeter 82 with computer-based recording units was picked for the present study. It is a precision rotational viscometer with concentric cylinders (inner cylinder ϕ 27 mm, slot width 1.5 mm) or a plate/cone measuring system. The appearance of the device is illustrated by Fig. 36.

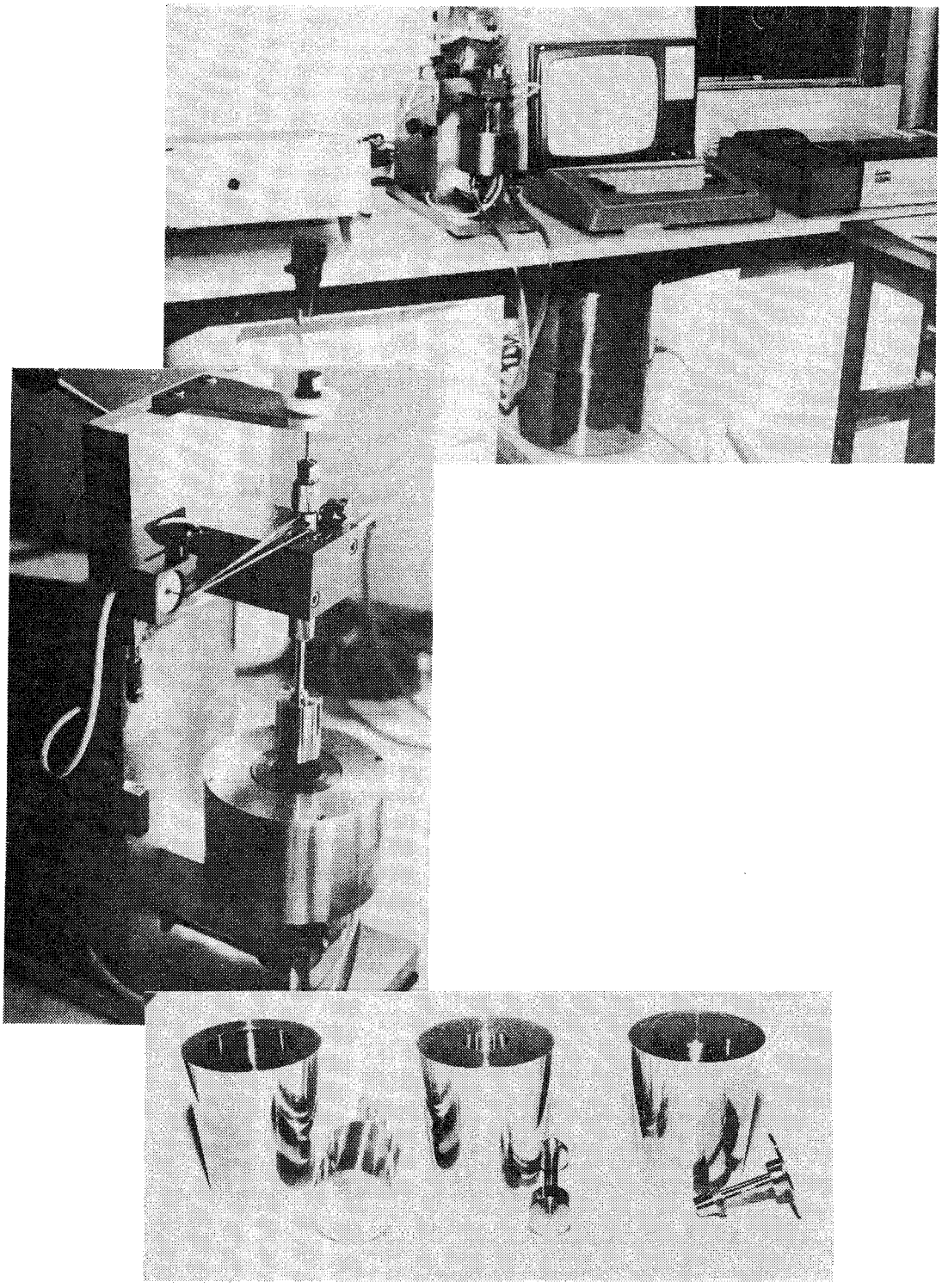

Fig. 36 The viscometer. Upper picture: from left to right: operational unit, viscometer, computer, and plotter. Central picture: the inner cylinder attached to the moment gauge is shown lifted out of the head with the rotational outer cylinder. Lower picture: cylinder sets and cone/plate set.

The viscometer is equipped with a heating facility so that tests can be run at elevated temperature. The present investigation comprised 20 tests at 20 ^{o}C and 3 tests at 40 ^{o}C. The viscometer was calibrated several times in the course of the investigation by using a Newtonian-type oil with a viscosity of 0.098 Pas at 25 ^{o}C.

The preparation of samples and subsequent measurements have been made according to the following program:

1. Dry MX-80 clay powder was mixed with the respective solution to the required water content in 500 ml vessels. Mechanical stirring and a few minutes ultra-sonic treatment were used to homogenize the mixture.

2. The carefully covered sample was allowed to rest for two days. Mechanical stirring was repeated once.

3. The sample was applied in the viscometer and left to rest for exactly 10 minutes. Rotation was then started and kept constant for 10 minutes with regular automatic evaluation of the shear stress and viscosity. A new sample was used for each of the five different rotation speeds that were applied. – The shear stress dropped in the course of the rotation and 10 min runs were found to yield practically constant shear stresses (τ, N/m^2 or Pa) which were plotted as in Fig. 35 against the rate of shear (D, s^{-1}).

The viscosity has been evaluated by applying the relationship:

$$\eta = \frac{R_y^2 - R_i^2}{4\pi h \cdot R_y^2 \cdot R_i^2} \cdot \frac{M}{\Omega} \qquad (5)$$

where η = viscosity

$R_y = R_i + \Delta r$

R_i = radius of cylinder

Δr = slot width

h = height of cylinder

M = recorded moment

Ω = rotation speed (rad/s)

The rotation speed ranged between 200 and 0.6 rad/s, depending on the choice of cylinder set and type of clay gel, except for the test with w=5000% where the highest speed was 630 rad/s.

The various tests, which concerned only low clay concentrations, are specified in Table 12.

Table 12. Specification of viscometer tests. Figures, except water contents and clay concentrations, represent test code numbers.

Water content	Clay conc.	Solution					
w,%	%	Aqua dest	"Allard"	NaCl $6\cdot10^{-2}$M	NaCl $6\cdot10^{-3}$M	$CaCl_2$ $3\cdot10^{-2}$M	$CaCl_2$ $3\cdot10^{-3}$M
300	33		20				
500	20	1	2	3	4	5	6
1000	10	7	8	9	10	11	12
2000	5	13	14	15	16	17	18
5000	2	19					

At a water content of 5000%, all solutions except the distilled water yielded flocculation and sedimentation. Lower water contents than slightly more than 500% gave certain difficulties in preparing homogeneous, air-free samples, and less accurate results. This is explained by the fact that this water content range corresponds to the Atterberg liquid limit of the bentonite. Higher water contents than 500% gave perfectly homogeneous samples and accurate determination of the properties of the correspondingly low clay concentrations that are representative of the front part of the bentonite clay penetrating rock joints.

Results

Fig. 37 illustrates the character of the relation between the rate of shear (D) and the shear stress for the dilute gels with a water content of 2000% (5000% for test no. 19). Table 13, which gives the evaluated τ_B- and η-values, shows that the shear resistance and viscosity of bentonite clay gels are strongly dependent on the water content. The shear stress drops only slightly when the rate of shear is reduced from the highest to the lowest value while the viscosity is very much increased. The latter effect, which is due to the very strong thixotropy of bentonite, makes it completely arbitrary to pick a specific η-value. In this report the viscosity corresponding to the lowest shear rate has been used as a reference value.

The water chemistry is important in the sense that Ca-rich solutions produce coagulation resulting in many large voids and local dense clusters which are poorly linked together. It is obvious that distilled water and synthetic ground water ("Allard" solution) yield similar rheological properties and that also very dilute gels show some resistance to shear. A water content of 2000-5000% is not representative of the main parts of the clay gel that penetrates a rock joint, but it certainly represents the outermost part of it.

As to the importance of a moderate temperature increase (20→40 ^{o}C) we find a slight influence only. This supports the assumption that in remolded, structurally incoherent clay particle assemblies represented here by the samples with water contents equal to or higher than 1000%, the shear strength as well as the viscosity are very moderately affected by temperature. The tests with bentonite having w=500% ("Allard" water), i.e. with more coherent clay, exhibit a stronger temperature dependence. Here, the viscosity dropped from about 800 Pas to about 580 Pas on heating from 20 to

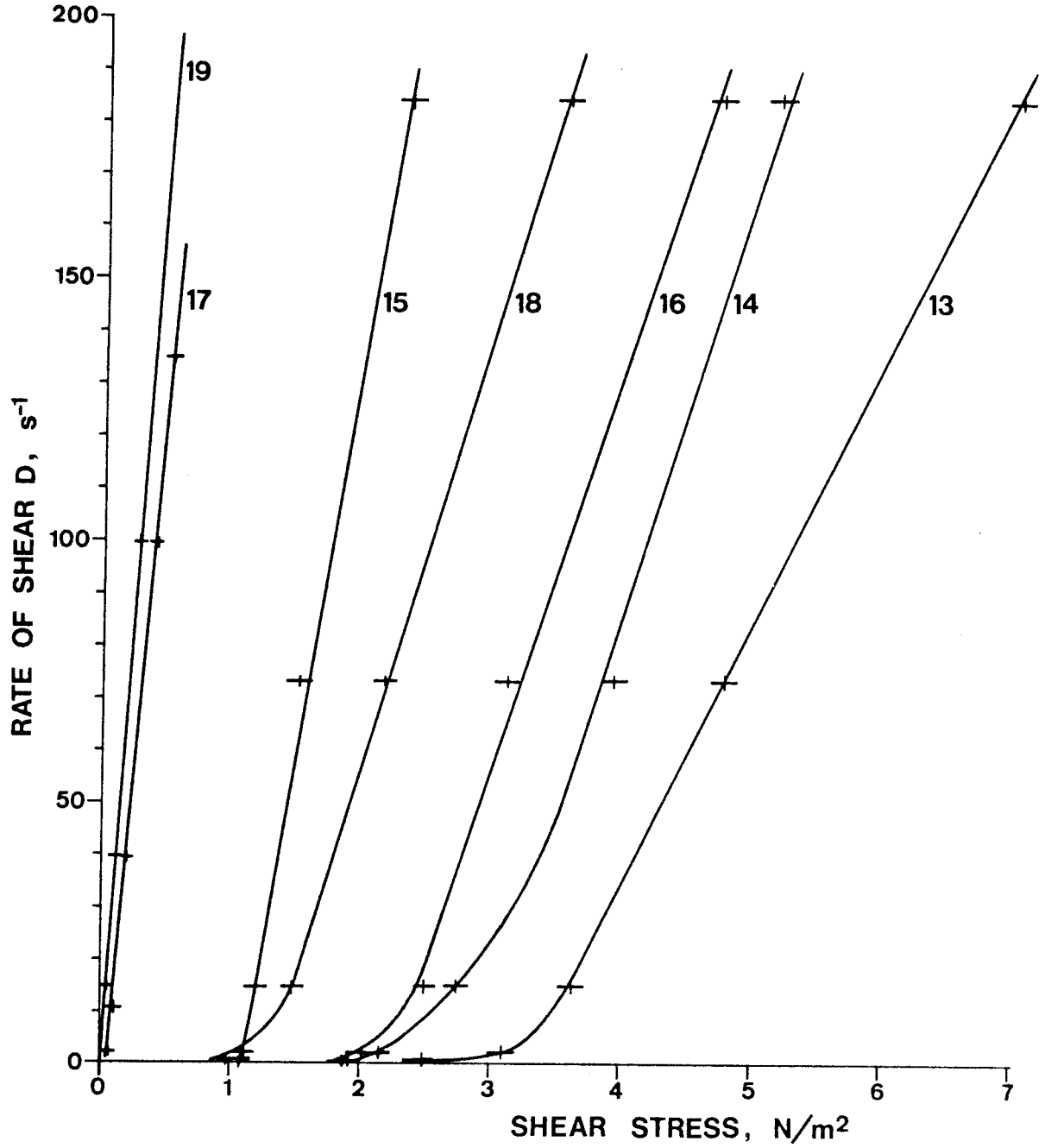

Fig. 37. Example of recorded τ/D relationships for MX-80 bentonite. Figures refer to test code numbers specified in Table 12.

Table 13. τ_B and η evaluated from the viscometer tests.

Water content %	Clay conc. w,%	τ_B Pa 22°C	η Pas 22°C	Solution	Test code no.
500		~900	750	Distilled water	1
1000	10	39	26		7
2000	5	3	3		13
5000	2	<0.1	<0.1		19
300	33	~1700	~18000	"Allard"	20
500	20	~1000	~800		2
1000	10	28	18		8
2000	5	3	2		14
500	20	~900	~240	$6 \cdot 10^{-3}$M NaCl	4
1000	10	24	17		10
2000	5	2	2		16
500	20	~750	~200	$3 \cdot 10^{-3}$M $CaCl_2$	6
1000	10	20	16		12
2000	5	1	1		18
500	20	~300	~110	$6 \cdot 10^{-2}$ NaCl	3
1000	10	6	5		9
2000	5	1	1		15
500	20	~20	~16	$3 \cdot 10^{-2}$M $CaCl_2$	5
1000	10	0.5	0.5		12
2000	5	0.1	<0.1		18

40 °C. Correspondingly, the shear resistance at the lowest rotation speed dropped from about 470 kPa to 340 Pa. The temperature effect on these gels after complete thixotropic strength regain, i.e. at lower shear rates, is expected to be higher.

5.2.3 Evaluation of particle bond strength

τ_B can be used for a rough estimation of the particle bond strength. Thus, assuming that all interparticle bonds are activated simultaneously and to the same extent, we obtain the maximum shear force of the individual bonds by dividing τ_B by the total number of bonds. This is an incorrect procedure in the case

of undisturbed, aggregated clay with the heterogeneous microstructure that is typical for natural clays [16], but it can be accepted for a completely remolded, homogeneous clay matrix such as the ones we presently consider. If the particles are assumed to be equally sized and distributed, their shape being taken as spherical (Stoke equivalents) with 0.15 μm diameter (cf. Fig. 2), we arrive at the approximate particle numbers per m^3: 10^{20} for w=500%, $5.4 \cdot 10^{19}$ for w=1000%, and $2.8 \cdot 10^{19}$ for w=2000%. Since the coordination numbers must be very different over this wide range of clay concentrations we will first consider only the most dilute gel and assume that each clay particle forms 3 contacts with neighboring particles. If it is further assumed that the particle distribution is uniform, which should be reasonable for distilled water and acceptable, possibly, for "Allard" water but not for stronger electrolytes, we arrive at the figure $2.8 \cdot 10^{13}$ contacts per m^2 cross section. For "Allard" solution, the maximum shear force S, or the individual bond strengh, will then be equal to τ_B=3 N/m^2 divided by the number of contacts, i.e. $S \sim 10^{-13}$ N. If we repeat the calculation for w=1000% and assume the slightly higher coordination number 4 (cf. [36]), S will be about $4 \cdot 10^{-13}$ N. The discrepancy between the two S-values is explained by the much improved degree of continuity of the particle network at the latter clay concentration which, in turn, means that the actual effective coordination numbers are related 1:5. Since this number can hardly exceed 4, the figure $4 \cdot 10^{-13}$N per contact is probably the most correct value. It is of the same order of magnitude as the lower limit of OSIPOV's range [17].

The particle bonds in the presently considered soft gels represent the ultimate, minimum strength to which probably only "long range" electrostatic attraction forces contribute. This suggests that as long as flocculation prevails in natural groundwater of low salinity the particle bond strength remains practically

constant although a reduction in clay concentration will yield separation and sedimentation of individual flocs. The latter effects are also caused by an increased salinity, which produces ubiquitary, "syneresis"-type contraction which happened in the viscometer testing of the more saline samples. Here, the particle bond strength actually increased through the contraction but the continuous gels were transformed into systems of large flocs. In nature, this would require flooding the repository area for many thousand years by a salt sea.

Flocculation with concomitant, spontaneous, separation of the flocs from the very soft clay gel front in rock joints may, theoretically, offer a possibility of rapid erosion by flowing water. The flocs may well be stable and not disintegrate, but they can be transported away from the gel front if their size is sufficiently small. This floc property has been thoroughly studied by a number of investigators who all seem to have arrived at the conclusion that individual clay particle behavior does not occur in practice[1)]. Thus, also in water with extremely low cation concentrations clay

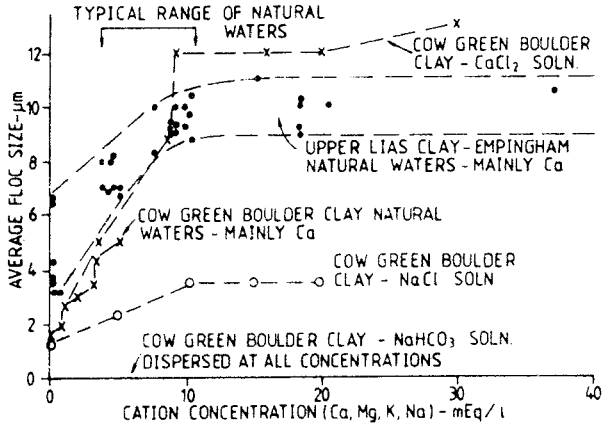

Fig. 38. Variation in clay floc size with water chemistry [37].

---

1) This is with the exception for the case of strong mechanical agitation in the presence of peptizing agents.

particles form flocs with an average size that exceeds 1 μm (Fig. 38), [37].

5.3 Drag forces

The flowing water exerts a drag force on particles constituting the clay gel. This force can be estimated by applying basic hydrodynamics in the follwing way. Assume that the particles are spherical and that water flows all around those particles which protrude from the expanding gel (Fig. 38).

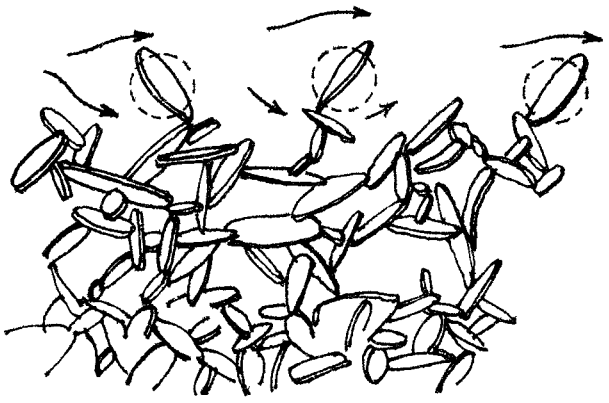

Fig. 39. Schematic view of clay gel front exposed to drag forces produced by flowing water.

Assuming further, as we do when applying Stoke's law for evaluation of the particle size from sedimentation tests, that the drag force can be expressed as:

$$F = k_1 \cdot \eta \cdot v \qquad (6)$$

where $k_1 = 3\pi d$ in the case of spherical particle shape

d = Stoke diameter

η = viscosity of the water

v = flow velocity

we arrive at the F-values given by Table 14 for particles with d in the interval 0.1 μm - 2 μm and water flow rates between 10^{-6} and $4 \cdot 10^{-4}$ m/s. These

figures represent the boundaries of the expected interval of flow rates in the joints of our rock model a few hundred years after sealing the repository (cf. Chapter 3.7.2). The calculated drag forces refer to the conservative, long term case of low rock temperature. At elevated temperatures the drag force would be smaller.

Table 14. Drag force F as a function of particle size d and water flow velocity v at 15 °C.

d, μm	v m/s	F, N
0.1	10^{-6}	$6.7 \cdot 10^{-16}$
0.5		$3.4 \cdot 10^{-15}$
1.0		$6.7 \cdot 10^{-15}$
2.0		$1.3 \cdot 10^{-14}$
0.1	10^{-5}	$6.7 \cdot 10^{-15}$
0.5		$3.4 \cdot 10^{-14}$
1.0		$6.7 \cdot 10^{-14}$
2.0		$1.3 \cdot 10^{-13}$
0.1	10^{-4}	$6.7 \cdot 10^{-14}$
0.5		$3.4 \cdot 10^{-13}$
1.0		$6.7 \cdot 10^{-13}$
2.0		$1.3 \cdot 10^{-12}$
0.1	10^{-3}	$6.7 \cdot 10^{-13}$
0.5		$3.4 \cdot 10^{-12}$
1.0		$6.7 \cdot 10^{-12}$
2.0		$1.3 \cdot 10^{-11}$

We can conclude from Table 14 that the drag force exerted on particles smaller than 0.5 μm, i.e. the large majority of the particle assembly, is less than about $4 \cdot 10^{-13}$ N when the flow rate is 10^{-4} m/s and that this force drops to less than $4 \cdot 10^{-15}$ N when the flow rate is only 10^{-6} m/s. This indicates that for most of the montmorillonite particles forming the gel front, one single bond is sufficient to balance the

drag forces and this suggests that groundwater erosion of the clay gel emanating from the deposition holes will be negligible. Isolated flocs can obviously be moved by the slowly flowing groundwater in the widest joints but we see that only a few bonds established between temporarily stationary neighboring flocs or to surface-active minerals in the rock matrix is sufficient to anchor the flocs. Due to this and to the large size of the flocs they will easily get stuck in the joints particularly where the aperture has minima. Bentonite loss through removal of flocs produced by an increased salinity will therefore be without importance.

The theoretical considerations thus indicate that groundwater erosion will be negligible in the presently discussed type of rock with the considered low hydraulic gradients. The validity of this conclusion remains to be evidenced, however, and efforts were therefore made to investigate the erosive effect in an experimental study using the pinhole test.

5.4 Pinhole tests

5.4.1 Equipment

The standard version of the permeameter cell was not chosen since it was considered to be unsuitable for tests with very dilute gels and very low gradients. A new device was therefore built (Fig. 39) which allows for heads of about 0.5 mm and hydraulic gradients as low as $1.3 \cdot 10^{-2}$.

The apparatus consists of a cylindrical cell with axially located in- and outlets. A water overpressure is applied by use of a large vessel, the water table of which is kept slightly higher than the inlet. It is maintained through the overflow principle, meaning that water cannot rise to a higher level above the inlet than where the outlet is. In most cases, percolation did not take place unless a temporary pressure rise had been applied, which required blocking of the overflow exit and installation of a standpipe (Fig. 40a).

The inlet is equipped with a 50 µm glass filter from which a ϕ 1 mm hole extends to the conical mouthpiece in the left part of the figure. At the outlet, a corresponding ϕ 1 mm passage leads to a pipe connection where the discharge is collected. The outlet is equipped with a narrow plastic tube with a moutpiece, shaped so as to eliminate surface tension effects, and a 10 ml glass collector, in series.

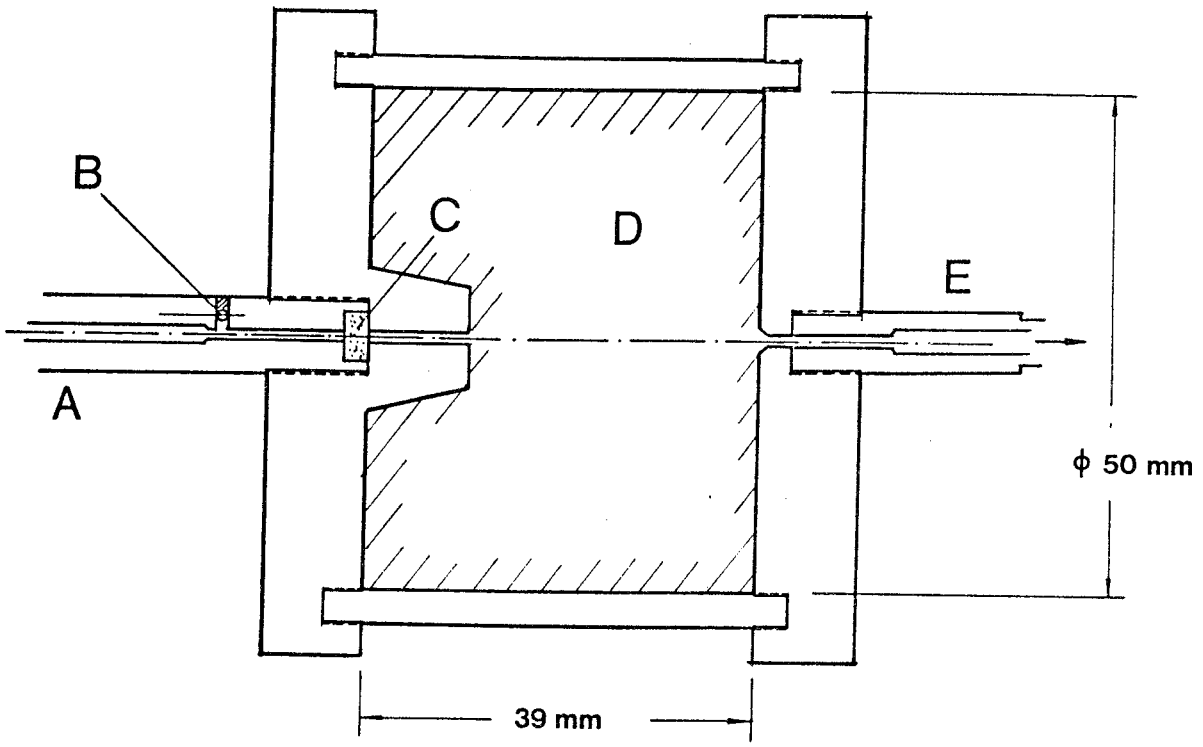

Fig. 39. Schematical section through the pinhole test device. A) Inlet mouthpiece, B) Overflow exit, C) Porous glass filter, D) Clay gel, E) Exit.

5.4.2 Test procedure and program

The cell is oriented with its axis in a vertical position and with the outlet pointing downwards for filling the cell with the gel. The cell is then closed by screwing the inlet base plate in position and turned so that the inlet points downwards. The exit mouthpiece is removed from the outlet base plate and the cell left to rest in this condition for 30 minutes so that the thixotropic gel is stabilized. The next step is to make the pinhole and this is achieved by slowly pushing a ϕ 1 mm metal tube ("pin") through the hole in the outlet base plate all the way through the clay and into the opposite passage. When the tube enters this passage a slight underpressure is applied so that its possible content of clay is removed, after which it is filled

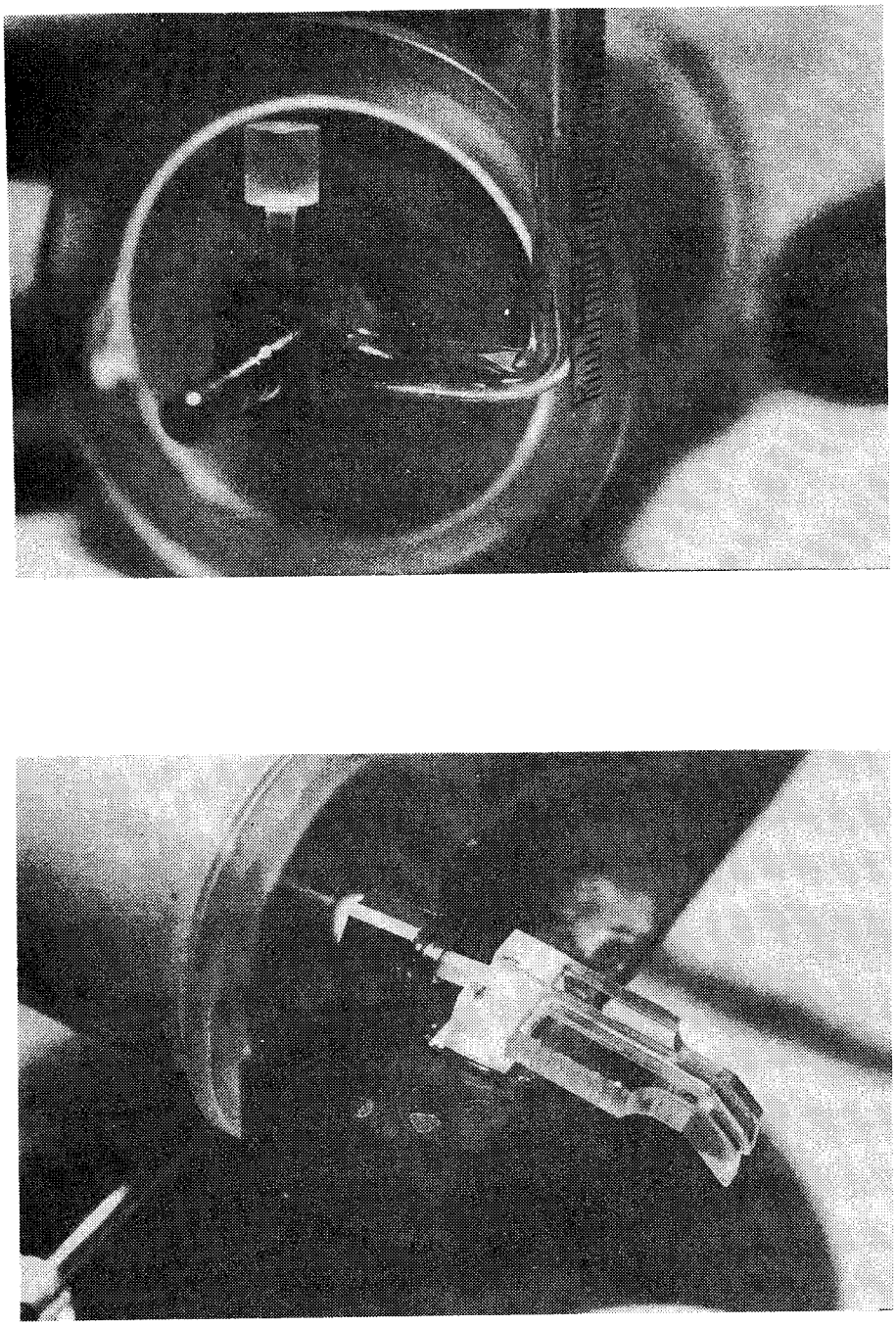

Fig. 40. Water inlet (upper picture) and outlet of the cell.

with the liquid which is intended for the test so that the filter becomes saturated. This is the case when water drops appear in the "overflow" hole at the inlet. The metal tube is then withdrawn and the outlet mouthpiece put in position with its axis horizontal, the inlet being connected to the large vessel. Some milliliters have to be allowed to flow through the cell to yield a condition of steady state before the collection of the discharge begins. In the present study, it was investigated with respect to its flow rate, and to its content of solid, eroded, clay particles.

The evaluation of the particle concentration of the discharge was made by drying the percolate at 105 ^{o}C for determination of the concentration of solids. This procedure gave values with an accuracy better than 0.001 g/l, which was quite sufficient for the present purpose.

The original program specified tests using MX-80 bentonite mixed with destilled water and "Allard" solution, with the gel concentrations 4% (w=2500%), 10% (w=1000%) and 20% (w= 500%). The actual concentrations had to be chosen so as to yield stable pinholes (Fig. 41). The lowest clay concentration when using distilled water was therefore 10% and the highest 23% (w=436%). With "Allard" solution the clay concentration could be as low as 5% (w=2000%). Pilot tests seemed to confirm the expected dispersiveness of smectite-rich clays, in the sense that once the pressure head exceeds a certain, critical value, the percolation rate become substantial. The chose of heads was therefore directed to the identification of this critical condition, the intention being to maintain the head for a sufficiently long period of time to make sure that steady state conditions prevailed. The initial pressure required to initiate flow was lowered to the minimum "critical" level immediately after flow was detected.

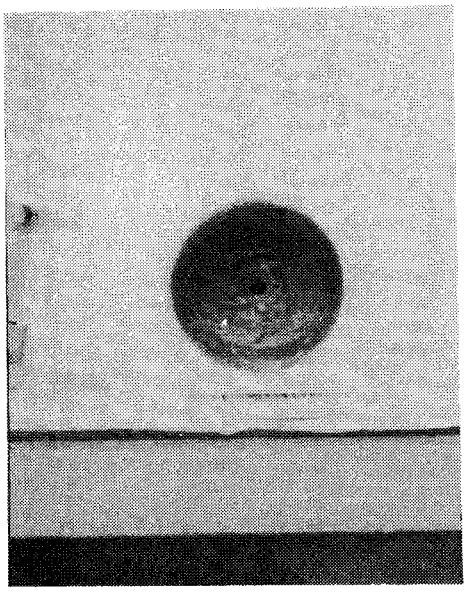

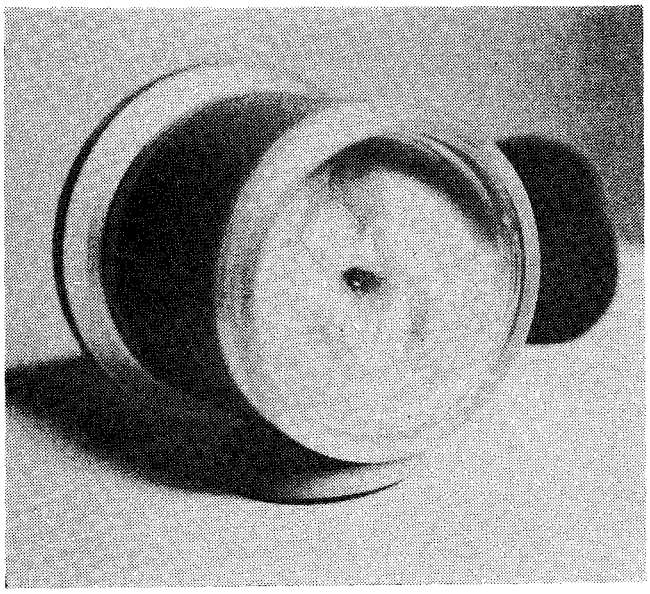

Fig. 41. Appearance of stable pinholes. Upper picture shows bentonite with w ~ 500%, lower picture w ~ 1000%

A common difficulty caused by the thixotropic properties of the montmorillonite/water gels was an observed irregular percolation with sudden intermittent stagnation and initiation of the flow. To avoid this, the pressure head had to be kept slightly higher than the critical value. Most test were run for at least ½ hour. The reproducibility was checked by running duplicate tests.

5.4.3 Results

The results from the pinhole tests are compiled in Table 15.

Table 15. Critical pressure heads and hydraulic gradients, and corresponding average flow rates

Water content w, %	Clay conc %	Critical head mm	Critical gradient	Av. flow rate m^3/s	Av. flow rate[1] m/s	Discharge conc %	Solution
435	23	4	10^{-1}	$7.0 \cdot 10^{-9}$	$9 \cdot 10^{-3}$	0.09	Aqua
435	23	4	10^{-1}	$7.7 \cdot 10^{-9}$	10^{-2}	0.07	dest
435	23	4	10^{-1}	$2.3 \cdot 10^{-9}$	$3 \cdot 10^{-3}$	0.07	
994	10	1.5	$3.8 \cdot 10^{-2}$	$3.8 \cdot 10^{-9}$	$5 \cdot 10^{-3}$	0.04	
994	10	0.5	$1.3 \cdot 10^{-2}$	$6.6 \cdot 10^{-9}$	$8 \cdot 10^{-3}$	0.006	
1000	10	0.5	$1.3 \cdot 10^{-2}$	$4.8 \cdot 10^{-9}$	$6 \cdot 10^{-3}$	0.05	"Allard"
1000	10	0.5	$1.3 \cdot 10^{-2}$	$2.3 \cdot 10^{-9}$	$3 \cdot 01^{-3}$	0.03	
1000	10	0.5	$1.3 \cdot 10^{-2}$	$5.5 \cdot 10^{-10}$	$7 \cdot 10^{-4}$	0.03	
2000	5	1	$2.6 \cdot 10^{-2}$	$3.0 \cdot 10^{-9}$	$4 \cdot 10^{-3}$	0.03	
2000	5	0.5	$1.3 \cdot 10^{-2}$	$2.0 \cdot 10^{-9}$	$2 \cdot 10^{-3}$	0.03	

1) Mass flow rate divided by theoretical cross section of the pinhole.

The data indicate that the pinholes were largely clogged in the course of the percolation and that the critical pressure was not the pressure required to produce substantial erosion, but to displace the slurry in the

pinhole. The erosive effect of flowing groundwater on the soft gels is thus not explicitely given by the table but a few relevant observations can still be made. Firstly, we see that the flow rates are 2 to 25 times as high as the maximum expected ones in the rock joints. At these high rates the drag forces should actually be able to rip off the large majority of the clay particles exposed to flowing water in the pinhole, and to produce a slurry with the same density as the gel (cf. chapter 5.3). Yet, we find that these high rates have only yielded discharge concentrations which are lower than 1 percent of the clay concentration of the respective gel.

The tests also serve as an illustration of the clogging effect of narrow apertures that is effected even by very dilute gels. As shown by the tests, gels with water contents as high as 500 to 2000% experience strong thixotropic strength regain if the drag forces produced by the water percolation drop below a critical level. Such gels are therefore expected to form stable plugs when they enter wider passages where the flow rate drops or when they get forced into wedge-shaped narrow passages which do not let individual flow through. Their soft character will probably not lower the average hydraulic conductivity of the rock very substantially but they will not migrate in the rock when low hydraulic gradients prevail.

The appearance of the discharge is illustrated by Fig. 42 which shows MX-80 bentonite dispersed in distilled water. While the percolates obtained from the tests with distilled water had the appearance of water with a sprinkle of milk, the ones from the tests with "Allard" water looked like pure water.

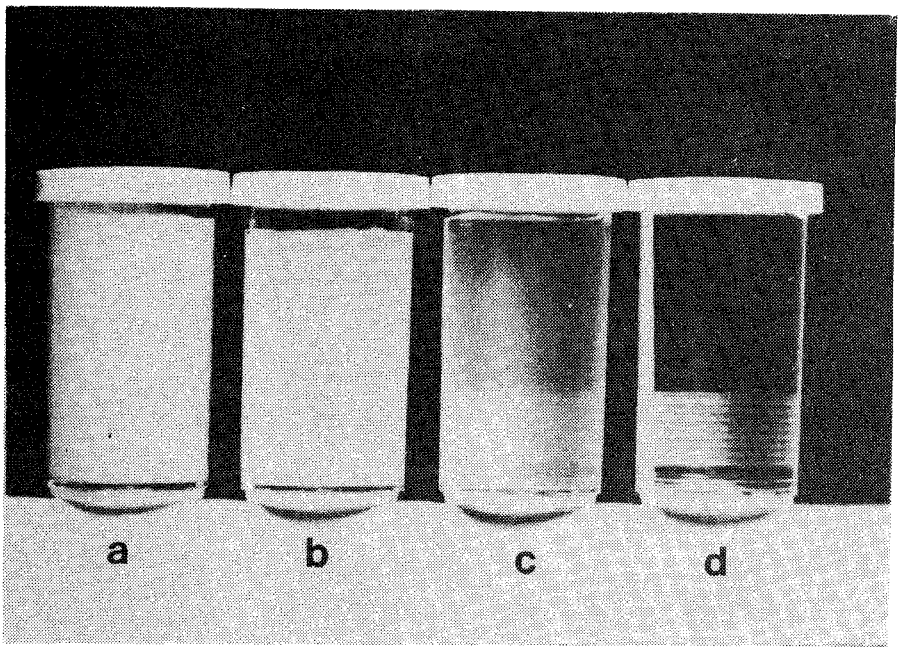

Fig. 42 MX-80 dispersions in distilled water. Clay concentrations are: a) 0.5%, b) 0.2%, c) 0.05%, d) 0%

6. DISCUSSION, CONCLUSIONS

6.1 Bentonite loss by clay expansion

The theoretical model of clay expansion into joints signifies that bentonite will enter the joints which traverse deposition holes. The rate is expected to be very slow, though, and this conclusion is also supported by the short-term experiments. In the normal case, i.e. where our rock model applies, bentonite will hardly reach beyond a few decimeters from the holes and the loss of clay from the holes will not affect, noticeably, the physical properties of the dense bentonite core that stays in them, at least in a 10^6 year perspective.

Existing joints may be widened by tectonic processes, by local stress fields produced by excavation processes, or by blasting, which makes it necessary to consider a more conservative but still realistic case. Such a case would be one in which rock mass displacement along steeply oriented joints induces frequent fractures by which one or several deposition holes will be located in a shear zone (Fig. 43). The shear displacement can be assumed to alter the initial joint assembly to a system of fractures with 5 times the number of initial joints and with 5 times the initial aperture of these joints. This would yield the figure 4.75 m^3 for the joint space with 3 m radius of influence instead of 0.19 m^3 in Table 5. If we apply the flow rate restrictions implied by the Poiseuille mechanism only to fractures with an aperture smaller than 1 mm, the estimated bentonite loss into the fractures is about 3 m^3 in 10^6 years. This quantity of bentonite, which thus seals the fractures and which is assumed to have an average density of 1.5 t/m^3, reduces the bulk density of the remaining highly compacted clay core from about 2.05 t/m^3 to about 1.9 t/m^3. We can see from Table 6 that this yields a drop in swelling pressure from 10-15 MPa to 3-7 MPa, and an increase in permeability from the interval $2 \cdot 10^{-14}$ - $8 \cdot 10^{-14}$ m/s to about $1.5 \cdot 10^{-13}$ m/s. These changes do not affect, substantially, the barrier effect of the bentonite in the deposition holes.

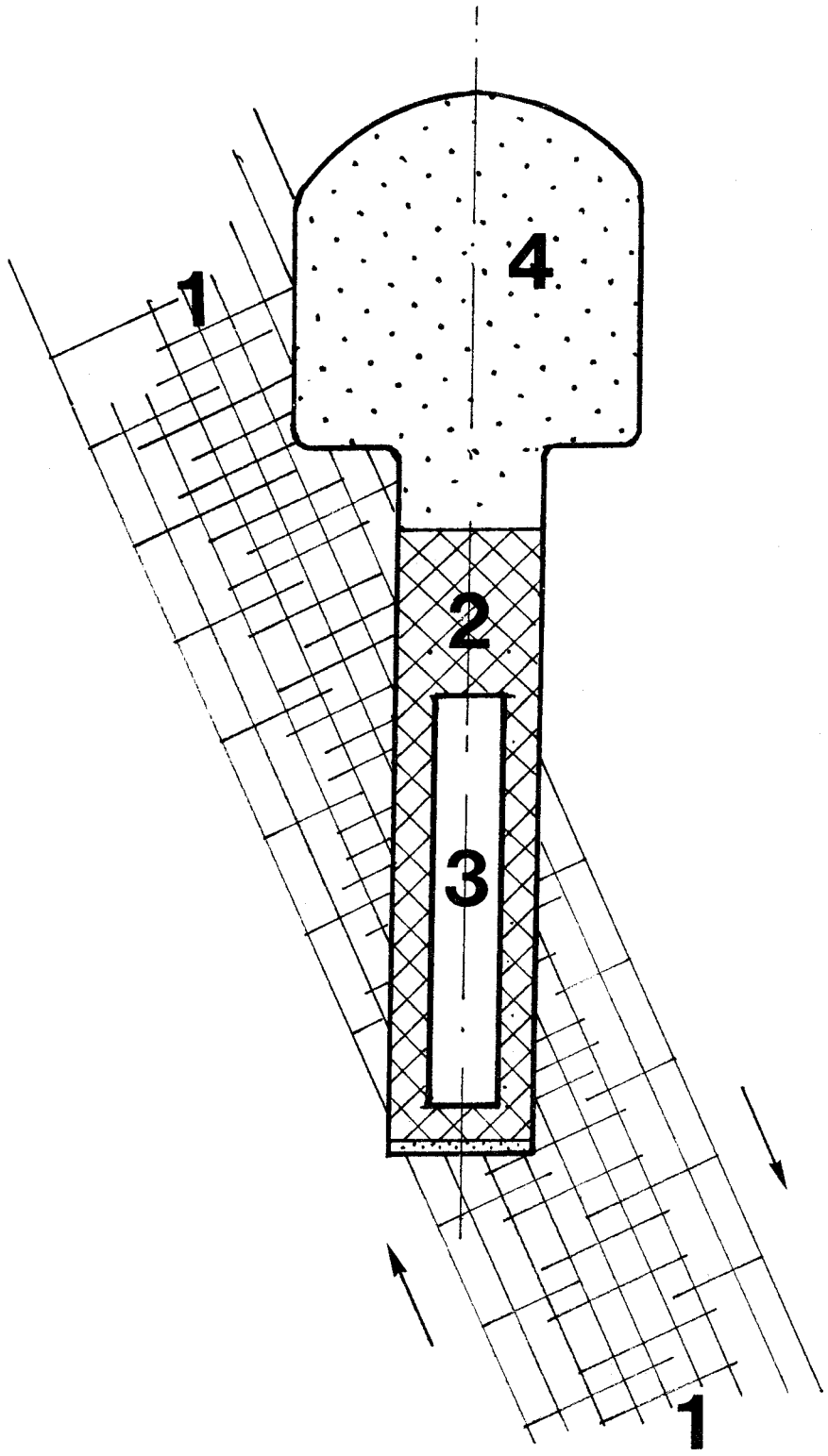

Fig. 43 Schematic picture of "worst case"; i.e. development of fracture-rich shear zone. 1) Shear zone, 2) Highly compacted bentonite, 3) Canister, 4) Sand/bentonite backfill.

Neither, it affects the settlement rate of the canisters in this clay, the predicted total settlement being less than 10 mm in 10^6 years [38].

6.2 Bentonite loss by erosion

Immediately after the application of the blocks of highly compacted bentonite and the canisters, the hydraulic gradients established in the rock during the several years long, preceding excavation period, are high. This yields temporary rapid water flow upwards in steeply oriented joints that are located close to the deposition holes. When the overlying tunnel has been backfilled, the gradients and the flow rates drop rapidly and approach a condition of steady state some decades after the sealing of the repository. Experience from the presently running Buffer Mass Test (Stripa Project) shows that erosion of the highly compacted bentonite in the initial phase is negligible. Nor will it affect, substantially, the clay that has penetrated into the rock joints of our rock model in later phases. The minor amount of very soft, flocculated clay that may be freed from the protruding gel front by slowly flowing water will not have any practically important effect on the remaining clay core in the deposition holes. Nor will it be an important carrier of radionuclides since it is expected to be held up by interaction with the rock crystal matrix in the joints and by physical obstacles.

If we consider the more severe case of the formation of a shear zone the situation is somewhat altered in the sense that such an event must be expected to set up considerable hydraulic gradients and to produce a large increase in hydraulic conductivity. Here, a large part of the clay gel that emanates from the deposition holes may be displaced far from the close vicinity of the deposition holes and this should affect the rate of expansion of the clay core. However, an increase in groundwater flow rate by 100 times, for instance, would still not erode the stiffer part of the penetrating clay

film, and would therefore not be able to produce a significant change in the rate of clay transfer from the deposition holes. This is in agreement also with the frequent observation that most clay-weathered zones with smectite minerals in surface-near rock show no sign of having been eroded in postglacial time.

6.3 Effect of clay migration on rock stability

It was early recognized that bentonite penetrating into joints does not only exert a radial pressure that helps to displace the bentonite but also a pressure normal to the joints which may affect the stability of the rock at the upper end of the deposition holes. These two pressures are equal since swelling on a macroscopic scale is isotropic, and since the fully developed swelling pressure will range between 5 and 15 MPa in the deposition holes it cannot be neglected. In practice it is taken into consideration by allowing for substantial breakup of the rock close to the tunnel floor as shown in Fig. 44. Zones marked "0" in this figure are rich in fractures caused by the blasting and they are apt to being affected by wedging through joint-penetrating bentonite. The penetration depth of bentonite, which is limited to about 2,8 m in 10^6 years, may well reach the outer edge of horizontally or only slightly inclined fractures in a few thousand years and may displace single blocks upwards. They can only emerge from the more or less conically shaped 0-zones and not from the rock mass to the left of line A-A in Fig. 44 where the rock pressure p_1 prevents open fractures to be developed. p_1 can be estimated at 15-25 MPa while p_2, which is the average effective overburden pressure, is expected to be about 8-10 MPa. The approximate pressure distribution in a horizontal fracture in the "0"-zone where the penetrating bentonite is supposed to have reached 0.5 m into the fracture, is illustrated in Fig. 45. It should be added here that the expected bentonite redistribution discussed in this context is taken into consideration by assuming the net bulk density value 2.05 t/m^3* instead of the theoretically derived value 2.10-2.15 t/m^3.

*ultimate bulk densities in KBS concepts 2 and 3

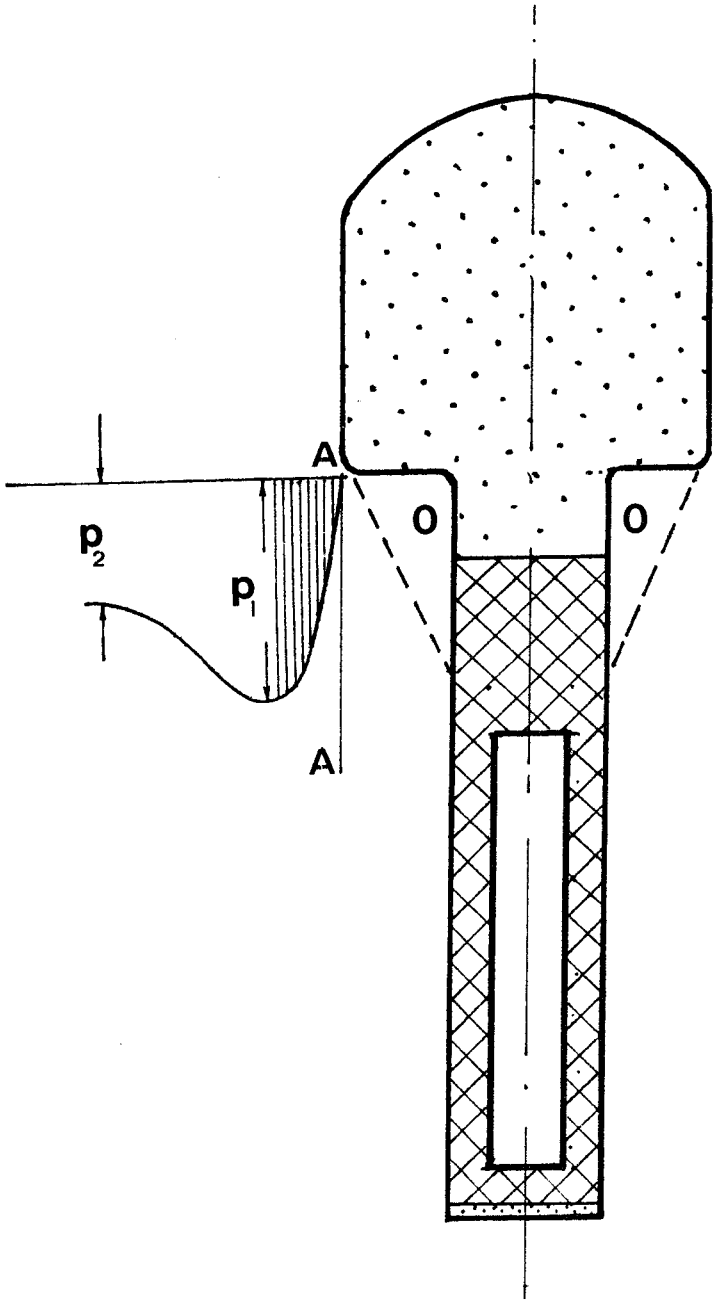

Fig. 44. Schematic cross section through deposition hole with potentially unstable rock zones "0" at the upper end of the hole

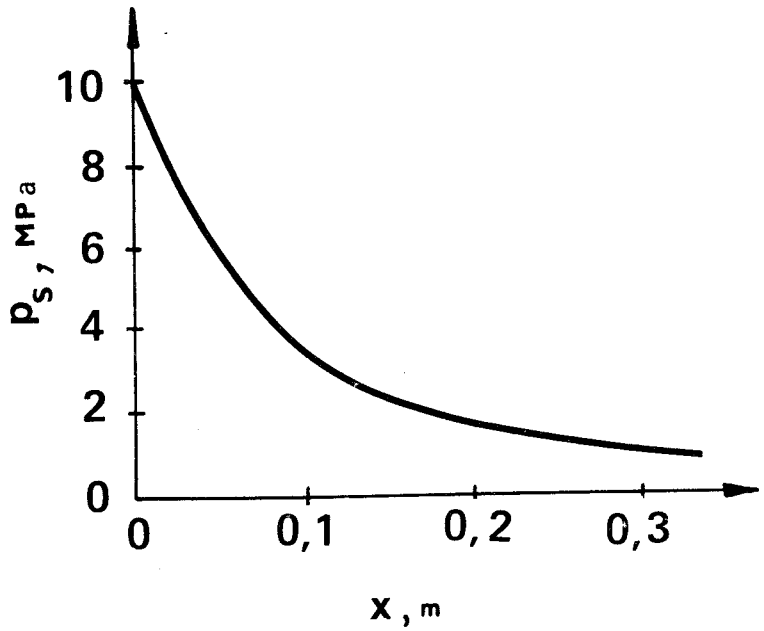

Fig. 45. Approximate pressure distribution in fracture with penetrating bentonite. x denotes distance from the boundary of the deposition hole

6.4 Beneficial effects of clay migration from deposition holes

It should be emphasized that, with the possible exception of the hypothetical formation of a shear zone, the penetration of clay into joints which traverse deposition holes yields valuable sealing of the joints. The clay filling thus displaces the groundwater flow from the interface between the highly compacted bentonite and the rock, and it yields a surface-active mass with substantial cation exchange capacity. It will also act as a protective zone for the clay in the deposition hole in the sense that changes in groundwater chemistry that are caused by external processes, such as pH-alterations or a strongly increased salinity, are buffered by the clay filling. It is clear, however, that its limited extension from the boundary of the deposition holes also limits these beneficial effects.

7. ACKNOWLEDGEMENTS

The present study was prepared by the Division of Soil Mechanics, University of Luleå, under contract with the SKBF/KBS. The Author wishes to express his sincere gratitude to the entire staff of our division for valuable help. Special thanks are given to Miss Kerstin Pousette, who set up the advanced viscometer equipment and carefully ran the tests, to Mr Thomas Forsberg, who was responsible for the granite-slot and pinhole tests and who made ingeneous test arrangements, as well to Mrs Kerstin Karlsson who made the typewriting and who has turned this activity into a noble art.

8. REFERENCES

1. M'EWEN, M.B. & PRATT, M.I. The gelation of montorillonite. Trans. Far. Soc. Vol. 53, 1957, pp. 535-547.

2. PUSCH, R. Water uptake, migration and swelling characteristics of unsaturated and saturated highly compacted bentonite. SKBF/KBS Teknisk Rapport 80-11, 1980.

3. NORRISH, K. The swelling of montmorillonite. Discuss. Faraday Soc. Vol. 18, 1954, 1954, pp. 120-134.

4. FORSLIND, E. & JACOBSSON, A. Clay/water interactions. Final Techn. Report. Eur. Res. Off. Contract Number DAJA 37-72-C-3894, July 1973.

5. FOSTER, W.R., SAVINS, J.G., & WAITE, J.M. Lattice expansion and rheological behavior relationships in water-montmorillonite systems. Clays and Clay Minerals, Proc. 3rd Nat. Conf. 1956, pp. 296-316.

6. PUSCH, R. Clay microstructure. Document D8:1970. Nat. Swed. Build. Res., Stockholm 1970.

7. PUSCH, R. Self-injection of highly compacted bentonite into rock joints. KBS Teknisk Rapport 73, 1978.

8. DERJAGUIN, B.W., & CHURAEV, N.V. Structural component of disjoining pressure. J. Coll. and Interface Sci., Vol. 48, 1974 (pp. 249-255).

9. van OLPHEN, H. Rheological phenomenon of clay soils in connection with the charge distribution on the micelles. Discuss. Faraday Soc. Vol. 11, 1951.

10. LAMBE, T.W. The structure of compacted clay. J. Soil Mech. a. Found. Div., Proc. ASCE, SM 2, vol. 84, Part 1, 1958.

11. FORSLIND, E. & DANIELSSON. Unpublished report. Swedish Concrete Institute, Stockholm, 1955.

12. RESENDIZ, D. Considerations of the solid-liquid interaction in clay-water systems. Proc. 6. Int. Conf. Soil Mech. a. Found. Engng., Vol. 1., 1965 (pp. 97-100).

13. ROSENQVIST, I.TH. Investigations in the clay-electrolyte-water system. Norg. Geot. Inst. Publ. No. 9, 1955 (p. 36).

14. OVCHARENKO, F.D., et. al. Investigation of the physico-chemical mechanics of clay-mineral dispersion. Israel Program for Sci. Translations, Jerusalem, 1967 (pp. 19-26).

15. ARNOLD, M. A study of thixotropic action in bentonite clay. Diss. Univ. Adelaide, Australia, 1967 (pp 30-31).

16. PUSCH, R. Rate process theory and clay micro-structure. Proc. IV Int. Conf. Soil Mech. a. Found. Engng., Spec. Session 9, Tokyo, 1977 (pp. 223-227).

17. OSIPOV, V.I. Structural bonds and the properties of clays. Bull. Eng. Geol. No. 12, 1975 (pp. 13-20).

18. van OLPHEN; H. An introduction to clay colloid chemistry. Interscience, New York, 1963.

19. LeBELL, J.C. Colloid chemical aspects of the "confined bentonite concept". SKBF/KBS Teknisk Rapport 97, 1978.

20. PUSCH, R. Bergmekanik. Almqvist & Wiksell, Stockholm, 1974 (p. 23).

21. LIDSTRÖM, L. Surface and bond-forming properties of quartz and silicate minerals and their application in mineral processing techniques. Acta Polytech. Scand. Vol. 75, 1968.

22. THORPE, R. Characterization of discontinuities in the Stripa granite time-scale heater experiment. Swedish-American Coop. Program on Radioactive Waste Storage in Mined Caverns in Crystalline Rock. Techn. Int. Rep. No. 20, 1979.

23. PUSCH, R. Water uptake and swelling of montmorillonitic clay seams in rock. Proc. Int. Soc. Rock. Mech. Montreux 1979, Vol. 1 (pp. 273-278).

24. PUSCH, R. Borehole sealing with highly compacted Na bentonite. SKBF/KBS Teknisk Rapport 81-09.

25. HANSBO, S. Consolidation of clay, with special reference to influence of vertical sand drains. Swed. Geot. Institute, Proc. No. 18, 1960.

26. PUSCH, R. Mineral-water interactions and their influence on the physical behavior of highly compacted Na bentonite. Can. Geot. Journal, Vol. 19, No. 3, 1982.

27. BRACKLEY, I.J.A. Swell pressure and free swell. Proc. 3. Int. Conf. Expansive Clays. Israel 1973, Vol. I.

28. MEADE, R.H. Removal of water and rearrangement of particles during the compaction of clayey sediments-Review. U.S. Geol. Surv. Prof. Paper 479-B, 1964.

29 PUSCH, R. Swelling pressure of highly compacted bentonite. SKBF/KBS Teknisk Rapport 80-13, 1980.

30. PUSCH, R. Permeability of highly compacted bentonite. SKBF/KBS Teknisk Rapport 80-16, 1980.

31. HOUWINK, R. Elastizität/Plastizität und Struktur der Materie. Verl. Theodor Steinkopf, Dresden u. Leipzig. 1958 (p. 353).

32. PUSCH, R. Inverkan av förhöjd temperatur på finkornig jord- förstudie. Byggdok. 32401, Anslagsrapport BFR 790827, (Statens Råd för Byggnadsforskning).

33. THORSLUND, P. Ordovician and Silurian strata at Kinnekulle. The Chasmops Series of the Kullatorp Core. Geol. Inst. Univ. of Uppsala, Bull. Vol. 32, 1948.

34. NICKEL, S.H. A rheological approach to dispersive clays. ASTM., STP 623, J.L. Sherard and R.S. Decker, eds. Amer. Soc. for Testing and Materials, 1977 (pp. 303--312).

35. YONG, R.N., SETHI, A.J., LUDWIG, H.P., & JORGENSEN, M.A. Physical chemistry of dispersive clay particle interaction. Am. Soc. Civ. Eng. Preprint 3379, 1978.

36. MITCHELL, J.K. Shearing resistance of soils as a rate process. J. Soil Mech. A. Found. Div., Proc. Am. Soc. Civ. Eng., SMI, 1964 (pp. 29-61).

37. VAUGHAN, P.R. & SOARES, H.F. Design of filters for clay cores of dams. ASCE Proc. Geotechnical Engineering Div. Journal 108 (1982): GT1, (pp. 17-31).

38. PUSCH, R. Stress/strain/time properties of highly compacted bentonite. SKBF/KBS Teknisk Rapport (In preparation).

LIST OF KBS's TECHNICAL REPORTS

1977-78

TR 121 KBS Technical Reports 1 - 120.
Summaries. Stockholm, May 1979.

1979

TR 79-28 The KBS Annual Report 1979.
KBS Technical Reports 79-01--79-27.
Summaries. Stockholm, March 1980.

1980

TR 80-26 The KBS Annual Report 1980.
KBS Technical Reports 80-01--80-25.
Summaries. Stockholm, March 1981.

1981

TR 81-17 The KBS Annual Report 1981.
KBS Technical Reports 81-01--81-16
Summaries. Stockholm, April 1982.

1983

TR 83-01 Radionuclide transport in a single fissure
A laboratory study
Trygve E Eriksen
Department of Nuclear Chemistry
The Royal Institute of Technology
Stockholm, Sweden 1983-01-19

TR 83-02 The possible effects of alfa and beta radiolysis on the matrix dissolution of spent nuclear fuel
I Grenthe
I Puigdomènech
J Bruno
Department of Inorganic Chemistry
Royal Institute of Technology
Stockholm, Sweden January 1983

TR 83-03 Smectite alteration
Proceedings of a colloquium at State University of New York at Buffalo, May 26-27, 1982
Compiled by Duwayne M Anderson
State University of New York at Buffalo
February 15, 1983

TR 83-04 Stability of bentonite gels in crystalline rock - Physical aspects
Roland Pusch
Division Soil Mechanics, University of Luleå
Luleå, Sweden, 1983-02-20

TR 83-05 Studies of pitting corrosion on archeological bronzes
Åke Bresle
Jozef Saers
Birgit Arrhenius
Archeological Research Laboratory
University of Stockholm
Stockholm, Sweden 1983-02-10

TR 83-06 Investigation of the stress corrosion cracking of pure copper
L A Benjamin
D Hardie
R N Parkins
University of Newcastle upon Tyne
Department of Metallurgy and Engineering Materials
Newcastle upon Tyne, Great Britain, April 1983

TR 83-07 Sorption of radionuclides on geologic media - A literature survey. I: Fission Products
K Andersson
B Allard
Department of Nuclear Chemistry
Chalmers University of Technology
Göteborg, Sweden 1983-01-31

TR 83-08 Formation and properties of actinide colloids
U Olofsson
B Allard
M Bengtsson
B Torstenfelt
K Andersson
Department of Nuclear Chemistry
Chalmers University of Technology
Göteborg, Sweden 1983-01-30

TR 83-09 Complexes of actinides with naturally occurring organic substances - Literature survey
U Olofsson
B Allard
Department of Nucluear Chemistry
Chalmers University of Technology
Göteborg, Sweden 1983-02-15

TR 83-10 Radiolysis in nature:
Evidence from the Oklo natural reactors
David B Curtis
Alexander J Gancarz
New Mexico, USA February 1983

TR 83-11 Description of recipient areas related to final storage of unreprocessed spent nuclear fuel

Björn Sundblad
Ulla Bergström
Studsvik Energiteknik AB
Nyköping, Sweden 1983-02-07